Mathematical Biosciences and Engineering

https://www.aimspress.com/journal/mbe

MBE, 23(2): 333–365.
DOI: 10.3934/mbe.2026014
Received: 31 July 2025
Revised: 23 October 2025
Accepted: 25 November 2025
Published: 06 January 2026

Research article

Incentives for self-isolation based on incidence rather than prevalence could help to flatten the curve: A modeling study

Giulia de Meijere[1] **and Hugo Martin**[2,*]

[1] Tampere Complexity Lab, Data Science Research Center, Tampere University, 33720, Tampere, Finland

[2] IRMAR, Université de Rennes, CNRS, IRMAR - UMR 6625, 35000 Rennes *and* INRAE, Agrocampus Ouest, Université de Rennes, IGEPP, Le Rheu, France. Now at Institut Denis Poisson (IDP), Université de Tours, 37000 Tours, France

* **Correspondence:** Email: hugo.martin@univ-tours.fr.

Abstract: In recent years, numerous advances have been made in understanding how epidemic dynamics are affected by changes in individual behaviors. We propose a Susceptible-Infected-Susceptible (SIS) based compartmental model to tackle the simultaneous and coupled evolution of an outbreak and of the adoption by individuals of the isolation measure. The compliance with self-isolation is described with the help of the imitation dynamics framework. Individuals are incentivized to isolate based on the prevalence and the incidence rate of the outbreak, and are tempted to defy isolation recommendations depending on the duration of the isolation and on the cost of putting social interactions on hold. We are able to derive analytical results on the equilibria of the model under the homogeneous mean-field approximation. Simulating the compartmental model on empirical networks, we also perform a preliminary check of the impact of a network structure on our analytical predictions. We find that the dynamics collapse to surprisingly simple regimes where either the imitation dynamics no longer plays a role or the equilibrium prevalence depends on only two parameters of the model, namely the cost and the relative time spent in isolation. Whether individuals prioritize disease prevalence or incidence as an indicator of the state of the outbreak appears to play no role on the equilibria of the dynamics. However, it turns out that favoring incidence may help to flatten the curve in the transient phase of the dynamics. We also find a fair agreement between our analytical predictions and simulations run on an empirical multiplex network.

Keywords: compartmental model; imitation dynamics; self-isolation; source of information; asymptotic behavior; transient phase; minimization of prevalence

1. Introduction

The survival and well-being of populations can be seriously threatened by the circulation of communicable diseases. At the same time, the very individuals concerned with the spread of a pathogen are often actively involved in the effort to mitigate the spread and to control the pathogen's health-care impact. Indeed, mitigation measures usually rely on the encouraged but voluntary adoption by individuals of attitudes that are expected to lower the probability of new infections, and thus benefit all. However, voluntary adoption as a behavioral decision is believed to be more than just a spontaneous immutable and homogeneous state of a population. Multiple surveys have identified individual factors (e.g., psychological, socio-economic) and message delivery factors (communication about the importance of a measure, and about the severity of the circulating pathogen) that influence whether a person can or will adopt a measure [1–4]. In addition to these factors, people form such decisions based on the influence of their social surroundings [5–7].

The coupled evolution of disease dynamics and mitigation behaviors has emerged as a vibrant research field, as evidenced by literature reviews published across a range of scientific communities, including mathematical modeling [8–12], physics [13, 14], public health [15, 16], and human behavior [17]. Two independent monographs [18, 19] further attest to the establishment of this line of research. However, the complex phenomenology that arises from this coupling remains only partially understood. Various approaches have been proposed to include human behavior into epidemiological models. Among them, the framework of imitation dynamics relies on the hypothesis that individuals carefully weigh their different options based on the observed payoffs of others before actively taking a side [20]. This framework has been used to model choices related to vaccinations [21–25], social distancing [26–29], mask-wearing [30, 31], and the use of insecticide-treated nets [32]. For certain diseases, seasonality plays a pivotal role, and is included within the mathematical models. However, even without such periodic modulations, the coupling between the dynamics of the disease and human behavior is able to generate oscillations as long as the population only partially complies with the mitigation measure in place. If individuals update their opinions sufficiently fast relative to the spreading rate of the disease, then the oscillations are either necessarily damped [33] or possibly sustained [21]. However, the scalar measure which represents the state of the outbreak that should be communicated or the rate of exposure to information that would be beneficial for mitigation are not yet thoroughly understood. In the present work, we propose to address these questions, with the aim of better orienting policy makers and communication during present and future outbreaks.

In the initial stages of a novel outbreak, efficient vaccines and drugs are rarely available and populations are forced to resort to non-pharmaceutical interventions (NPI) in order to slow down the spread of the disease. Depending on the disease [34], the most efficient NPI to mitigate the spread might vary. However, self-isolation of known infected individuals is a standard NPI that relies on the complete interruption of social interactions over a limited period of time, and was heavily relied upon during the COVID-19 pandemic. Although the measure would ideally only isolate individuals while and if they are infectious, logistical reasons often force healthy or recovered individuals to spend time in complete isolation from the community. Some modeling works have accounted for this type of inefficiency [35,36], while others have allowed individuals to enter and break self-isolation at any time [37].

Here, we focus on the impact of an imitation dynamic on the efficacy of the self-isolation measure. To do so, we build on a compartmental model introduced in [38] that explicitly accounts for the follow-

ing inefficiencies in its implementation: partial adoption, and pre- and post-isolation infections. Partial adoption described in the model allows individuals to decide not to isolate at all, as opposed to several other models for isolation or quarantine where quarantine is not a choice [39,40]. For individuals who comply, pre-isolation infection due to a delayed start of quarantine can be a consequence of unawareness of the infected status (asymptomatic or pre-symptomatic infection, unspecific symptoms, absence of accurate diagnostic tests) or of logistical difficulties with interrupting the current levels of activity (e.g., work-related). Post-isolation infection due to the overhasty termination of the isolation period can instead be a consequence of 'isolation fatigue' [41] or of isolation recommendations which require individuals to isolate for a duration that does not always cover the entire infectious period of patients.

In the present work, we make two substantial additions to this model. First, we introduce the possibility for individuals exiting quarantine before full recovery to re-enter the community with a reduced infectiousness. This lowered contribution to the force of infection can be attributed either to the adoption of precautionary measures (e.g., social distancing, mask-wearing) or to the pathogen load diminishing as the host's immune response progresses [42,43].

Second and more importantly, while in [38], the probability of deciding whether to isolate or not is constant, we here let it evolve over time. The decision of an individual is made after carefully pondering the cost of isolating and the responsibility towards the community, based on some information on the state of the outbreak at a given time. In the framework of imitation dynamics, the level of prevalence is the most common information that is used by agents to make their decision. However, both the prevalence and incidence are considered as the main indicators in epidemiology for the description of the state of an outbreak [44]. In the present work, we include both indicators to compare their effect on the efficacy of the isolation measure and the dynamics of the disease, when the population self-regulates the levels of adoption (see [45] for another model with a composite source of information). We expect the dynamic and reactive nature of the self-isolation measure to affect the phenomenology of the coupled behavior and disease dynamics in a different way compared to measures such as vaccinations and mask wearing [21,33]. While self-isolation has previously been modeled in combination with imitation dynamics (albeit in a different context, [46]), to our knowledge, it has not yet been studied in the presence of such dual source of information.

We analyze the equilibria of our model and perform a local stability analysis. We find five equilibria and no bi-stable state. Surprisingly, the type of information used (i.e., prevalence or incidence) does not affect the equilibrium values or their stability regions. However, prioritizing incidence over prevalence when making decisions may reduce the peak height of the epidemic curve, while marginally contributing to the total number of cases. This bias remains neutral under low basic reproduction numbers or the limited volatility of opinions. In contrast, if the disease propagates fast and individuals update their strategy at a quick pace, then emphasizing on incidence-based data can help contain the overall impact of the disease.

In Section 2, we introduce our model in its homogeneous mean-field formulation and describe its implementation on a two-layers network. Section 3 is devoted to the investigation of the dependence of stationary points of the dynamics and their local stability on the model parameters; additionally, we explore the impact of a sparser and more heterogeneous network structure on our analytical conclusions through simulations on an empirical network. Finally, in Section 4, we discuss our results and comment on perspectives for future work.

2. Modeling framework

2.1. ODE model

2.1.1. Disease dynamics

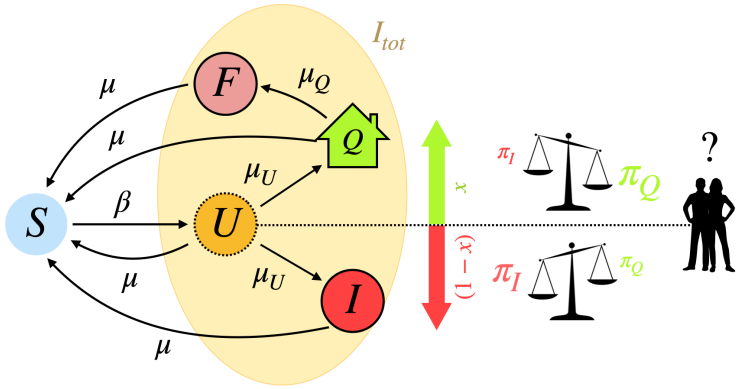

Figure 1. Schematic description of the compartmental model for an SIS-like epidemic evolution with an imitation dynamic that affects the probability that individuals cooperate with the isolation measure.

We build a compartmental model based on the standard Susceptible-Infected-Susceptible (SIS) epidemic model [47]. Let S denote the compartment of susceptible individuals who may contract an infectious disease. Here, the standard infected compartment of the SIS model is split into four distinct compartments—U, Q, I and F—to distinguish contagious from 'harmless' (because isolated) infected individuals.

With infection rate β and conditional to the contact between a susceptible and a non-isolated infected individual, newly infected individuals enter the compartment U of infected and undecided agents. We assume the standard homogeneous mean-field formulation of the probability of a contact between a susceptible and an infected individual. Individuals in the undecided compartment are infectious and have yet to decide whether or not to isolate (e.g., being unaware of their infected status or for logistical reasons). The spontaneous transition out of the undecided compartment occurs with the decision rate μ_U. Then, individuals either enter the isolated compartment Q with the compliance probability x or the still infectious compartment I with the complementary probability $1-x$. Individuals in the Q compartment are assumed to be perfectly isolated from the community. Although we describe the self-isolation of known infected individuals and not preventive quarantine, we call the isolation compartment Q to refer to the already existing literature on SIQS models [39,40,48–50]. Quarantined individuals can exit the Q compartment to enter yet another infectious compartment F (fatigued) - a transition that spontaneously occurs with the rate μ_Q. While individuals in compartment I who refuse to comply with the isolation measure are as contagious as individuals in compartment U, fatigued individuals in compartment F are conferred a decreased infectiousness $\beta(1-\varepsilon)$ to account for a potential increased awareness after the isolation period (resulting in protective behaviors such as mask wearing and social distancing) or a lower pathogen load due to the natural course of the infection. Although the rest that individuals get during isolation might help them to recover faster, we neglect it in the present

framework and consider that the time to recovery is identical on average, regardless of the decision made by individuals, and more in general regardless of the path they undertake in the flow diagram. To ensure this, direct transitions from compartments U, Q, I or F back to the susceptible compartment S occur with the same rate μ (see Appendix A). Note that undecided individuals may recover before ever making a decision. This happens when the recovery rate is much higher than the decision rate and corresponds to one limit where our model reduces to the standard SIS model.

Overall, the fraction of individuals in each compartment undergoes the following dynamics:

$$\begin{cases} \dot{S} &= -\beta S\,(U + I + (1-\varepsilon)F) + \mu(U + Q + I + F) \\ \dot{U} &= \beta S\,(U + I + (1-\varepsilon)F) - (\mu + \mu_U)U \\ \dot{Q} &= \mu_U x U - (\mu + \mu_Q)Q \\ \dot{I} &= \mu_U(1-x)U - \mu I \\ \dot{F} &= \mu_Q Q - \mu F, \end{cases}$$

with the assumption that demographic changes are negligible, which translates into $S+U+Q+I+F = 1$. For convenience, let I_{tot} denote the total prevalence (i.e., $I_{\text{tot}} = U + Q + I + F$).

2.1.2. Coupled disease and opinion dynamics

To make the here-above model for isolation more realistic, we let the probability x that undecided individuals comply with the isolation measure to be another variable of the model which evolves in time. We assume that an individual can either be a *cooperator* or a *defector*, depending on whether or not the individual undergoes self-isolation when aware of being infected. Now, the real number x can be understood as the fraction of cooperators in the population. In addition, people are assumed to dynamically change their opinion on self-isolation based on the comparison between the payoff of their own strategy and the payoff of the alternative strategy, which is in the fashion of the imitation dynamics framework [13, 21, 51]. Overall, the variable x undergoes the following dynamics:

$$\dot{x} = \sigma x(1-x)(\pi_Q - \pi_I),$$

where σ is the rate at which individuals challenge their opinion, and π_Q and π_I are the payoffs associated to the adoption (cooperation) or not (defection) of the isolation measure, respectively.

In the present imitation dynamics framework, we are able to account for the deterioration of compliance over longer isolation periods by making the payoff of cooperation decay with the duration of quarantine. More precisely, we model the cost to comply as the product of the daily cost to self-isolate multiplied by the average duration of isolation:

$$\pi_Q = -k \cdot \frac{1}{\mu + \mu_Q}.$$

The parameter k can be thought of as a straightforward monetary loss from being unable to commute to work, a burden from reorganizing housework, or a social cost from not seeing relatives and friends. A detailed derivation of the average time spent in compartment Q is provided in Appendix A.

In contrast, the payoff associated with defecting is assumed to decay with the prevalence I_{tot} and the incidence $\beta(1 - I_{\text{tot}})(I_{\text{tot}} - Q - \varepsilon F)$, with respective weights k_p and k_i:

$$\pi_I = -k_p I_{\text{tot}} - k_i \beta(1 - I_{\text{tot}})(I_{\text{tot}} - Q - \varepsilon F).$$

Combining both payoffs, the time evolution of the proportion of cooperators in the population reads as follows:

$$\dot{x} = \sigma x(1-x)\left(k_p I_{\text{tot}} + k_i\beta(1-I_{\text{tot}})(I_{\text{tot}} - Q - \varepsilon F) - \frac{k}{\mu+\mu_Q}\right).$$

Note that we assume that the fraction of cooperators is homogeneously distributed across all compartments. In particular, this implies that someone's current opinion is not affected by learning they are infected.

2.1.3. Final system of equations after nondimensionalization

Before conducting the mathematical analysis, we nondimensionalize our system by relying on the fact that the time of recovery provides a natural timescale μt for the system. Let $\mathcal{R}_0 := \frac{\beta}{\mu}$ be the basic reproduction number, which is also defined as the average number of secondary cases for each primary infected case in an otherwise susceptible population. After rescaling the time by μ, the final system reads as follows:

$$\begin{cases} \dot{I}_{\text{tot}} &= \mathcal{R}_0(1-I_{\text{tot}})(I_{\text{tot}} - Q - \varepsilon F) - I_{\text{tot}} \\ \dot{U} &= \mathcal{R}_0(1-I_{\text{tot}})(I_{\text{tot}} - Q - \varepsilon F) - (1+u)U \\ \dot{Q} &= uxU - (1+q)Q \\ \dot{F} &= qQ - F \\ \dot{x} &= \kappa x(1-x)\left(pI_{\text{tot}} + (1-p)\mathcal{R}_0(1-I_{\text{tot}})(I_{\text{tot}} - Q - \varepsilon F) - \frac{c}{1+q}\right), \end{cases} \tag{2.1}$$

where we have introduced the following:

- the relative decision-making rate (exit from compartment U), denoted $u := \frac{\mu_U}{\mu}$;
- the relative isolation-breaking rate (exit from compartment Q), denoted $q := \frac{\mu_Q}{\mu}$. Note that since the average time spent in isolation is $\frac{1}{\mu+\mu_Q}$, we can say that the average time for recovery is $q+1$ longer than the average time spent in isolation. Therefore, the mathematical condition $q > 0$ implies an infectious period always longer, on average, than the isolation period;
- the normalized opinion update rate $\kappa := \frac{\sigma(k_p+k_i)}{\mu}$;
- the relative importance given to prevalence when deciding whether to isolate or not, denoted $p := \frac{k_p}{k_p+k_i}$;
- the normalized daily cost of self-isolation $c := \frac{k}{\mu(k_p+k_i)}$.

Table 1. Summary of the final nondimensionalized model parameters.

Symbol	Name	Plausible range	Reference
$\mathcal{R}_0 \in (0,\infty)$	Basic reproduction number	$(0.3, 6)$	[52, 53]
$\varepsilon \in [0,1]$	Level of protection of infectious fatigued individuals	$(0.05, 0.95)$	[54, 55]
$u \in (0,\infty)$	Ratio of the decision-making rate over the recovery rate	$(0, 5)$	
$q \in (0,\infty)$	Ratio of the isolation-breaking rate over the recovery rate	$(0, 2)$	
$\kappa \in (0,\infty)$	Rescaled rate of opinion update	$(0, 50)$	
$p \in [0,1]$	Relative importance given to prevalence in the 'Defect' strategy	$[0, 1]$	
$c \in (0,\infty)$	Rescaled cost to self-isolation	$(0, 3)$	

When $x(t = 0) = 0$ or $u \to 0$, we recover the SIS system of equations. Instead, the case where $\kappa = 0$ is identical to the Isolation-Delay-Fatigue (IDF) model introduced in [38], where the compliance probability x is constant in time. In this paper, we only consider non-negative values for the parameter κ.

The parameter p of the model accounts for the relative importance of prevalence and incidence in the decision making of individuals. Fully tailoring compliance with isolation on the epidemic prevalence targets the containment of prevalence-related quantities, such as the hospital saturation levels and mortality. On the other hand, fully relying on incidence focuses on the probability of new infections, hence a refusal to isolate if there are either already too many infected individuals (the chances of meeting a susceptible individual whom they might infect are low) or still too few infected individuals (they would be among the few people isolating).

A schematic description of the compartmental model is provided in Figure 1 and the parameters used in the nondimensionalized model are summarized in Table 1.

2.2. Simulations

The mean-field equations for the imitation dynamics can arise from different implementations of the underlying stochastic dynamics. We simulate the dynamics using a Gillespie optimized algorithm [56] alongside the help of the Quasistationary State method, which was proven to be an efficient way of solely considering surviving runs in simulations of absorbing phase transitions [57].

We distinguish two stochastic implementations that we call 'one way' and 'two ways'. The 'two ways' implementation allows a change in strategy, even if the other strategy has a lower payoff. It sees the change in strategy just like an infection event, whereby an individual 'infects' a neighbor and makes it adopt its strategy. However, if the payoff of the explored strategy is much lower than the one of the original strategy, then the 'infected' individual quickly tends to transition back to its original strategy. Instead, the 'one way' implementation only allows the transition if the difference of payoffs between the two strategies is advantageous. In both implementations, the strategy changes are only performed if the strategy of the individuals who change is still carried by some (> 1) individuals in the population.

We compare the performances of the two designed implementations in terms of their error (i.e., deviation from the ordinary differential equations (ODE) model, and in terms of their execution times). More precisely, for each implementation, we simulate the time series of U, Q, I, F, and x on a complete network of $N = 500$ nodes. Averaging over a given number of runs, we obtain a time series for each compartment, and compute the 'combined mean error' as the sum of the absolute value of the difference between these time series and ODE predictions over all time steps and compartments. In Figure 2a, we compare the distribution of 50 combined mean errors for both implementations and for different numbers of runs. For both implementations, the error of simulations run on a complete network decays with the number of runs. However, we find that the error of the 'two ways' implementation decays more slowly. This is a consequence of the fact that the 'two ways' implementation allows quickly reversed and thus 'inefficient' transitions, whereby individuals change their strategy even though the new strategy incurs a lower payoff. In Figure 2b, we show the comparison between the distributions of execution times for each implementation. As a consequence of its inefficient transitions, the 'two ways' implementation appears to be also consistently slower in execution times compared to the 'one way' implementation. Moreover, these conclusions appear to persist on a network structure where the

stochastic implementation no longer perfectly agrees with the ODE predictions.

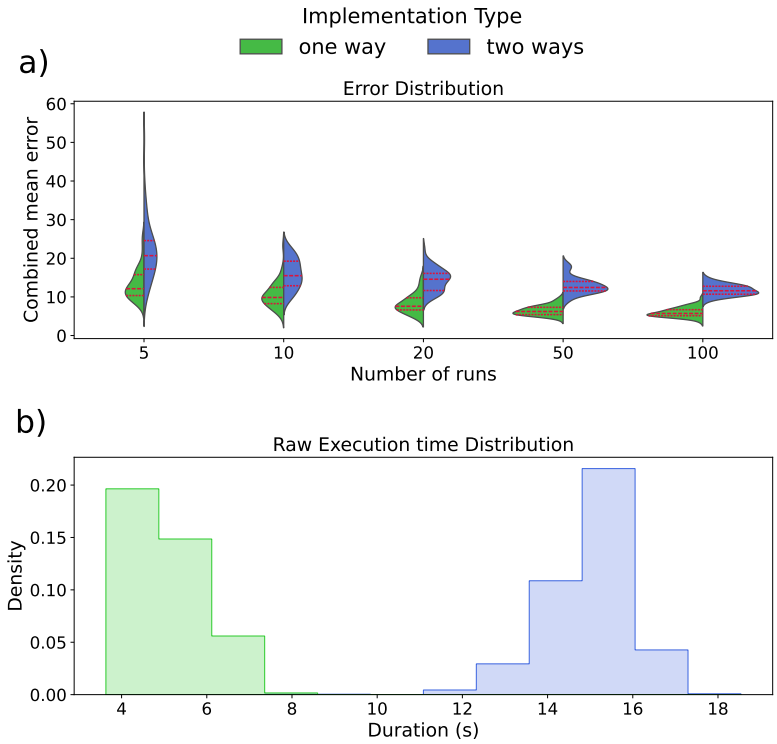

Figure 2. The 'one way' implementation is more efficient than the 'two ways' implementation. We compare the performance of both implementations on a complete network of size $N = 500$ until time 20. The other parameters are $\mathcal{R}_0 = 5$, $u = 4$, $q = 0.25$, $c = 0.5$, $p = 0.7$, $\kappa = 10$, and $\varepsilon = 0.5$, with the initial values $U(0) = I_{\text{tot}}(0) = 0.05$, $Q(0) = F(0) = 0$, and $x(0) = 0.01$. A total of 1000 runs were performed, and the associated error and execution time were stored. a) Violin plots of the distribution of 50 combined mean errors for the 'one way' (green) and the 'two ways' (blue) implementations, and for different numbers of runs. The red lines are the median (dashed) and the lower and upper quartiles (dotted). b) Distribution of the execution time for both the implementations.

Since the two approaches are both consistent but the 'one way' implementation is more efficient, results are here-after only shown for the 'one way' implementation.

Our model describes two spreading phenomena that occur on two distinct network layers. Thus we consider two different networks: one for the behavioral influence of individuals and one for the physical proximity (see for example [58] for a similar setting). For the empirical network structure, we consider data that was collected as part of the Copenhagen network study (CNS) [59, 60], which was a study that involved more than 700 students from a university in Copenhagen. Multi-layer temporal data was harvested over a period of four weeks through the mobile phones of the participants. Among other signals, the physical proximity of the students was estimated via Bluetooth signal strengths, and information about their Facebook friendships was also recorded. For the propagation of the synthetic disease, we use the `copenhagen/bt` Bluetooth dataset. Instead, for the layer where the adoption of measures propagates, we consider the `copenhagen/facebook` Facebook network. We assume that if

the number of nodes differs from one layer to the other, then it is a consequence of missing data and not a consequence of the inactivity of some nodes in either of the layers. The multi-layer network is aggregated over the entire observation period, and interactions between individuals are assumed to be unweighted and undirected.

3. Results

A stability analysis of the nondimensionalized ODE model (System (2.1)) reveals that the system has two disease-free equilibria as well as three endemic equilibria, which are distinguishable by the fraction of cooperators in the population. The equilibria of the dynamics and their conditions of stability shed light on the role played by pre-isolation and post-isolation infections, partial compliance, increased awareness after isolation, source of information and volatility of opinion. Moreover, simulating the stochastic dynamics of the present compartmental model on a network structure suggests a fair agreement with analytical results, although oscillations found in the ODE model may be damped faster on the network.

3.1. ODE model: equilibria and stability

The technical details of the assessment of the local asymptotic stability are postponed to Appendix B. In a nutshell, the procedure involves the following: (i) identifying the equilibria of the model; (ii) computing the Jacobian matrix associated with System (2.1); (iii) plugging the equilibria into the Jacobian matrix; and (iv) finding the eigenvalues.
Two of the equilibria correspond to disease-free situations (i.e., characterized by $I^*_{\text{tot}} = 0$ and thus also $U^* = Q^* = F^* = 0$). Consequently, the equilibria only differ by the level of compliance, which can only take two values. On the one hand, if $x^* = 1$, which corresponds to a scenario with full compliance, then we call the equilibrium Disease-Free with Full Compliance (DFFC). This equilibrium is unconditionally unstable. On the other hand, if $x^* = 0$, the equilibrium is called Disease-Free with No Compliance (DFNC), and is locally asymptotically stable if and only if $\mathcal{R}_0 \leqslant 1$. Indeed, in the absence of a threat, the incentive to self-isolate vanishes, which leads to the complete absence of cooperators in the population.

Since the other equilibria correspond to endemic situations, we assume $\mathcal{R}_0 > 1$ from this point onward. We are able to derive the equilibrium values of the fractions of individuals in compartments U, Q, I, and F along with the share x of cooperators in the population. In the stationary limit, the fractions of individuals in compartments U, Q, and F can be expressed as functions of x^* and I^*_{tot} as follows:

$$\begin{cases} U^* &= \frac{1}{1+u} I^*_{\text{tot}} \\ Q^* &= \left(1 - \frac{1}{1+u}\right) \frac{1}{1+q} x^* I^*_{\text{tot}} = \frac{u}{1+u} \frac{1}{1+q} x^* I^*_{\text{tot}} \\ F^* &= \left(1 - \frac{1}{1+u}\right)\left(1 - \frac{1}{1+q}\right) x^* I^*_{\text{tot}} = \frac{u}{1+u} \frac{q}{1+q} x^* I^*_{\text{tot}}, \end{cases} \tag{3.1}$$

where the stationary values x^* and I^*_{tot} solve the following two equations:

$$\begin{cases} \frac{1}{\mathcal{R}_0} &= (1 - I^*_{\text{tot}})\left(1 - \frac{u}{1+u} \frac{1+\varepsilon q}{1+q} x^*\right) \\ 0 &= x^*(1 - x^*)\left(I^*_{\text{tot}} - \frac{c}{1+q}\right), \end{cases} \tag{3.2}$$

under the assumption that $\kappa > 0$. We are left with the computation of the equilibrium values of x^* and I^*_{tot}.

Provided x^* lies in $[0, 1]$, the first line of System (3.2) gives the following:

$$I^*_{\text{tot}}(x^*) := 1 - \frac{1}{\mathcal{R}_{x^*}}.$$

where $\mathcal{R}_{x^*}$ reads as follows:

$$\mathcal{R}_{x^*} := \left(1 - \frac{u}{1+u}\frac{1+\varepsilon q}{1+q}x^*\right)\mathcal{R}_0. \tag{3.3}$$

In the case of no compliance (i.e., $x^* = 0$ ('No Compliance', ENC)), this expression reduces to the following standard SIS result:

$$I^*_{\text{tot}} = 1 - \frac{1}{\mathcal{R}_0}.$$

If full compliance is reached (i.e., $x^* = 1$ ('Full Compliance', EFC)), then the equilibrium prevalence is as follows:

$$I^*_{\text{tot}} = 1 - \frac{1}{\mathcal{R}_1}.$$

The parameter $\mathcal{R}_1$ can be understood as the basic reproduction number of a SIQS model with an extra compartment for fatigued individuals (pre- and post-isolation infections are modeled but partial adoption is not).

Finally, in case $0 < x^* < 1$ ('Partial Compliance', EPC), the second equation of System (3.2) yields a simple dependence of the equilibrium prevalence on the model parameters:

$$I^*_{\text{tot}} = \frac{c}{1+q}, \tag{3.4}$$

and the first equation provides the following equilibrium share of compliers:

$$x^* := \frac{1+u}{u}\frac{1+q}{1+\varepsilon q}\left(1 - \frac{1}{\mathcal{R}_0\left(1 - \frac{c}{1+q}\right)}\right). \tag{3.5}$$

Equating this expression to 0 and to 1 provides the stability conditions for the ENC and EFC equilibria, as well as the equations for the boundaries that separate the stability regions. It is worth to note that none of the equations depends on the initial conditions (except the conditions $\kappa > 0$ and $x(0) \in (0, 1)$).

All the results regarding the large time asymptotics of the model are summarized in Table 2.

3.2. The equilibrium prevalence reduces to a surprisingly simple dependence on the model parameters

We refer the reader to Figure 3 for heatmaps of the equilibrium prevalence across a variety of parameter combinations. Both the parameters p of the source of information (prevalence vs incidence) and κ of the volatility of opinions are omitted as they do not affect the equilibria. Indeed, at equilibrium, the incidence $\mathcal{R}_0(1 - I_{\text{tot}})(I_{\text{tot}} - Q - \varepsilon F)$ equals the prevalence I_{tot}, and the two contributions of the source of information cancel each other out.

Note that the intertwined evolution of disease and compliance with the self-isolation measure results in a surprisingly simple set of equilibria. In the two regimes 'Full Compliance' and 'No Compliance', the dynamics collapses to one where the imitation does not play any role. Instead, in the third and last regime, namely 'Partial Compliance', the equilibrium prevalence reduces to a very simple function of only two model parameters: the (rescaled) cost of isolation c and the relative isolation-breaking rate q.

Surprisingly, in this regime, the prevalence does not depend on the delay to enter isolation (through u) nor on the level of caution of individuals at the exit from isolation (through ε). Rather, delay and level of caution affect the equilibrium level of compliance x^* and the stability conditions of this regime. In 'Partial Compliance', being more careful to start the isolation period promptly (a larger u) or to limit risky behaviors after the isolation period (a larger ε) does not restrain the outbreak size, but makes the containment more efficient, which allows the same equilibrium prevalence I^*_{tot} with a lower overall compliance of the population x^*.

In the absence of changes in the adoption of the isolation measure, these two parameters are instead expected to always affect the equilibrium prevalence, unless there is no compliance at all. In Appendix C, we compare analytical predictions in the presence and in the absence of changes in compliance. We show that under the trivial condition where the static level of adherence of the population is given by the equilibrium level of adherence, the equilibrium prevalences are identical. Moreover, depending on the comparison between the initial level of adherence $x(t = 0)$ and the equilibrium level of adherence x^*, we can predict whether the dynamics with higher rates of imitation will generate consistently higher or lower prevalences in the transient phase.

3.3. Optimal isolation duration

We find that an optimal isolation period emerges. We typically observe that the equilibrium prevalence is minimized by an intermediate isolation duration, thereby balancing the trade-off between the increased efficacy of extended isolation periods against the importance of widespread adoption for breaking transmission chains.

For a sufficiently large c and sufficiently low q (long isolation duration), the system is in the 'No Compliance' regime and the prevalence is independent of q. When q reaches the value at which it leaves the 'No Compliance' regime to enter the 'Partial Compliance' regime, the prevalence starts monotonically decaying with an increasing q: shortening the isolation duration allows one to increase the population's adoption levels and to better contain the spread of the pathogen. However, above a certain value of q, the system changes the regime once again and enters the 'Full Compliance' regime, where further increasing q (and shortening the isolation duration) makes the prevalence grow again: the adoption level reaches a ceiling, and shorter isolation periods can only be detrimental for the containment of the disease spread. Thus, the value of q that minimizes the equilibrium prevalence is the value of q that separates the 'Partial Compliance' and the 'Full Compliance' regimes. This value of q corresponds to the longest isolation period such that everyone complies. Still, a lower prevalence is always achieved for longer optimal isolation periods. The improvement offered by choosing the optimal duration might be modest (Figure 3, bottom panels) or dramatic (top right panel, for rather low costs c), depending on the celerity to enter isolation u and on the caution after exiting isolation ε.

However, such an optimal isolation period does not exist in all regions of the space of parameters. In particular, it is necessary that the cost of quarantine is sufficiently large. Indeed, if c is too small ($c < 1 - \frac{1+u}{\mathcal{R}_0}$), then a large fraction of the population cooperates, and there is no further compliance to

be won by shortening the isolation period.

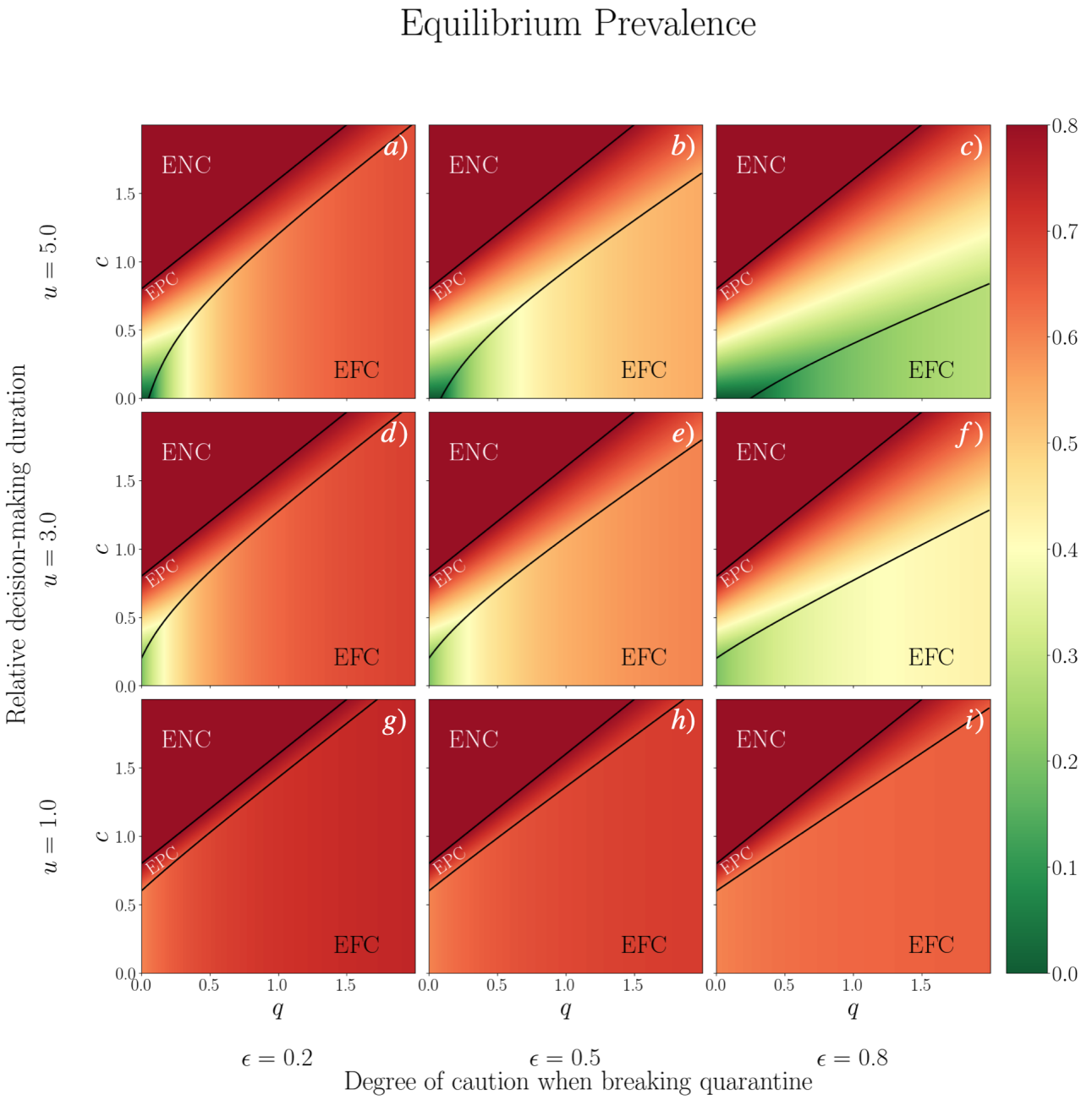

Figure 3. Equilbrium prevalence. Heatmaps of the equilibrium prevalence depending on the cost c of quarantine, the lack of coverage q of the infectious period by quarantine, the celerity of entrance in isolation u, and the degree of caution ε when breaking quarantine. The limits separating the ENC and EPC regimes, as well as the ones separating the EPC and EFC regimes are shown (black lines). The basic reproduction number is set to $\mathcal{R}_0 = 5$.

In Figure 4, we show the impact of different choices of the cost c of quarantine on the existence of an optimal isolation duration. In Figure 4a, we focus on the central panel of Figure 3, and propose

the exploration of several trajectories in the c vs q space. First, we consider different constant costs c and make the parameter q vary. Then, we postulate various correlations between c and q, and explore their impact on the equilibrium prevalence. Since we expect that the perspective of a long isolation duration heavily weighs on complying individuals, we propose two minimal ways in which the cost of isolation decays with q (light green and blue lines). However, we can also imagine that the perceived cost of isolation is the largest for very short isolation periods. Thus, we also provide one example of the behavior of the system under such an unrealistic scenario (red line). In Figure 4b, we see how the choice of the cost affects the existence of an optimal isolation period as well as the range of values of prevalence that can be achieved.

Table 2. Properties of the equilibria associated to System (2.1). Only the values of I^*_{tot} and x^* are displayed, since the other fractions can readily be deduced from their values, using System (3.1). 'Existence conditions' are obtained by requiring $I^*_{\text{tot}}, x^* \in [0,1] \times [0,1]$.

Name	Abbr.	Value of x^*	Value of I^*_{tot}	Existence	Stability
Disease-Free with No Compliance	DFNC	0	0	$\mathcal{R}_0 \leqslant 1$	$\mathcal{R}_0 \leqslant 1$
Disease-Free with Full Compliance	DFFC	1	0	$\mathcal{R}_1 \leqslant 1$	Never
Endemic with No Compliance	ENC	0	$1 - \frac{1}{\mathcal{R}_0}$	$\mathcal{R}_0 > 1$	$1 - \frac{1}{\mathcal{R}_0} \leqslant \frac{c}{1+q}$
Endemic with Partial Compliance	EPC	$x^* \in (0,1)$ given by (3.5)	$\frac{c}{1+q}$	$\mathcal{R}_0 > 1$, $\frac{c}{1+q} \in \left(1 - \frac{1}{\mathcal{R}_1}, 1 - \frac{1}{\mathcal{R}_0}\right)$	At least for κ 'small enough'
Endemic with Full Compliance	EFC	1	$1 - \frac{1}{\mathcal{R}_1}$	$\mathcal{R}_1 > 1$	$\frac{c}{1+q} \leqslant 1 - \frac{1}{\mathcal{R}_1}$

3.4. The source of information plays a role in the transient phase of the dynamics

Although the relative importance given to prevalence compared to incidence plays no role on the equilibria, we find that it affects the initial transient phase of the dynamics. More specifically, it appears that the peak of the prevalence is always minimized by a smaller value of p (i.e., a preference given to the incidence rate as a source of information as opposed to the prevalence). In Figure 5, we show how increasing the parameter p in the 'Partial Compliance' regime leads to a higher peak prevalence without significantly affecting the average prevalence over the entire time window considered (i.e., the temporal average). Similarly, the authors of [46] found that a parameter of perceived cost could have a large effect on the height of a single wave epidemic peak, while affecting the final epidemic size in a negligible way. In our model, it appears that it is equivalent to use prevalence or incidence as a source of information under certain conditions, while it is beneficial to consider incidence in others. This effect is the strongest for faster dynamics (i.e., higher basic reproduction numbers and higher volatility of opinions). This result is surprising in the sense that using incidence as the indicator of the responsibility of individuals towards the community allows them, in principle, to refuse to isolate when the prevalence is excessively large. However, the incidence grows faster at the beginning of an outbreak

compared to the prevalence, which allows for a swifter reaction of the population to the outbreak. We stress that the difference between the curves remains small in most of the cases. Additionally, we show that these conclusions hold when simulating the model on the multi-layer empirical network described in Section 2.2.

3.5. The decision process only affects undecided individuals

Our model demonstrates the capacity for sustained oscillations under specific conditions.

The coupling of disease and behavior dynamics in models has been shown to produce oscillations, particularly in the presence of an imitation dynamic and a sufficiently high opinion update rate [21,37]. However, there are nuances in the nature of the oscillations that can arise. For instance, a model for vaccination [21] identifies a threshold above which oscillations are sustained, a finding that contrasts with a model for mask-wearing [33], where only damped oscillations are observed. This discrepancy can be attributed to the delayed effect of a change in strategy on the disease dynamics. In [33], when individuals change strategy, their new behavior has an immediate impact on the transmission rate. Conversely, in [21], a parent's decision to vaccinate their child is irreversible once immunization has occurred at birth. Thus, a change in their opinion can only impact the system through the birth of another child.

Our current model adopts a similar philosophical stance regarding decision irreversibility. When individuals enter the U compartment, they make a definitive choice regarding self-isolation. Any potential regret concerning this strategy necessitates recovery from the current infection, followed by a subsequent reinfection, before a new decision can be made.

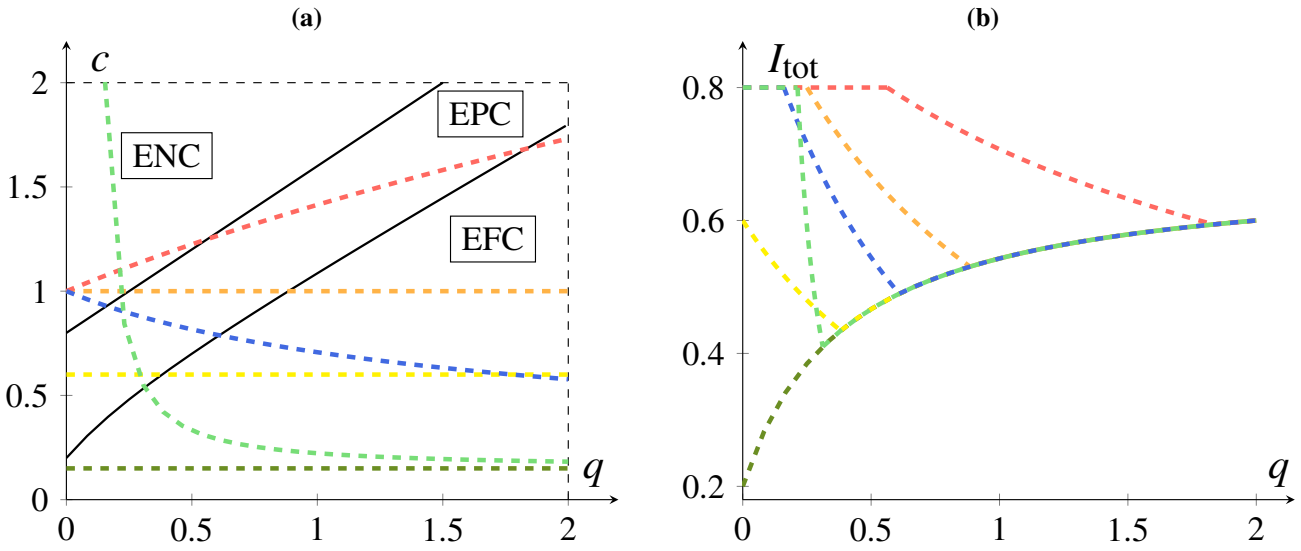

Figure 4. Conditions for an optimal duration of quarantine. a): Different choices of the parameter c: $c = 0.15$ (dark green), $c(q) = 0.1 * \exp\left(0.4 * \left(1 + \frac{1}{q}\right)\right)$ (light green), $c = 0.6$ (yellow), $c(q) = \sqrt{1+q}$ (blue), $c = 1$ (orange) and $c(q) = \frac{1}{\sqrt{1+q}}$ (red). b): Equilibrium prevalence as a function of q when considering the values of c shown in panel a. Parameter values: $\mathcal{R}_0 = 5$, $u = 3$, $\varepsilon = 0.5$.

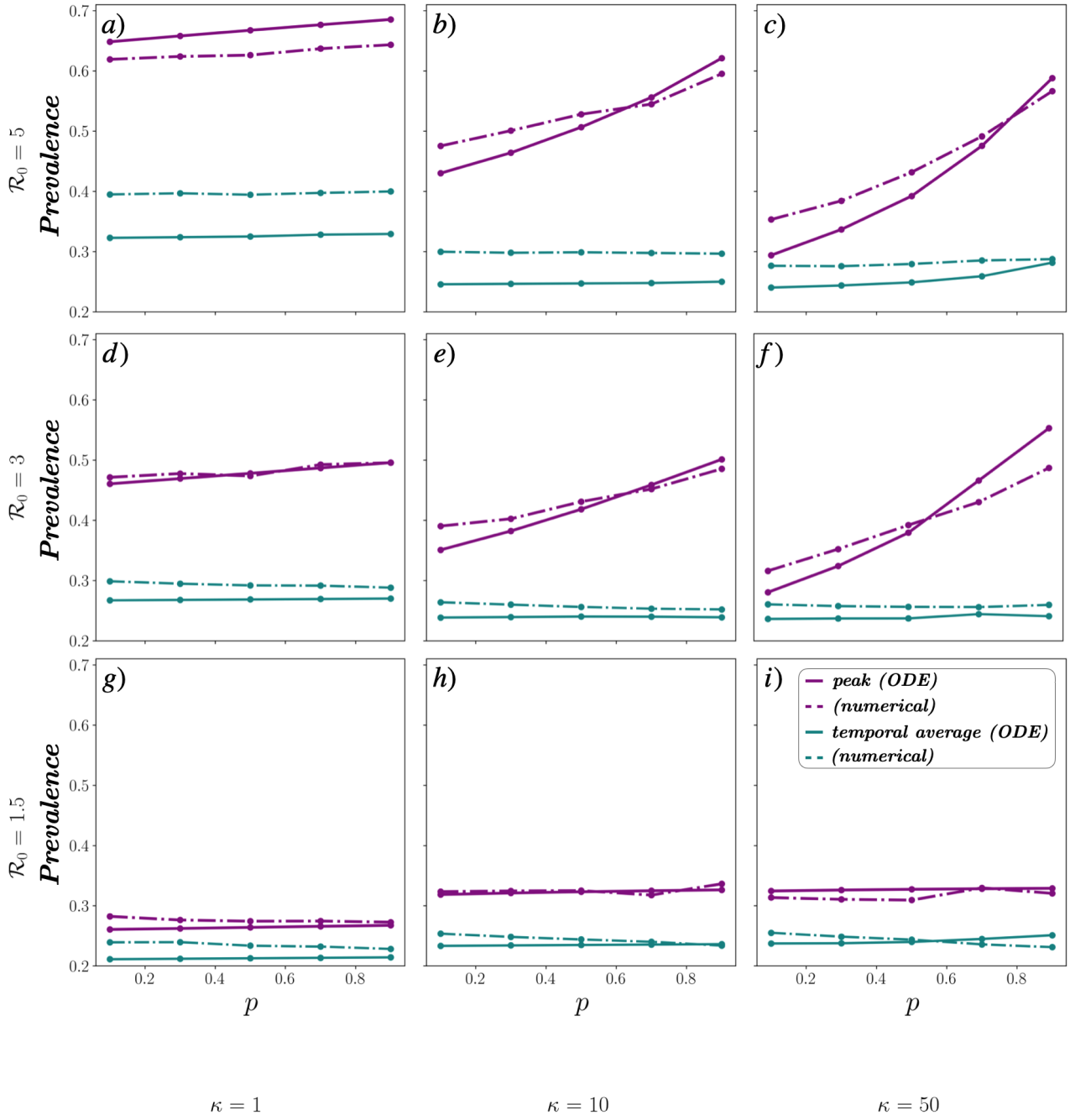

Figure 5. The incidence as an indicator of the state of the outbreak can help to flatten the curve. We show the value of the peak prevalence (purple) and its temporal average (dark cyan) as functions of the parameter p for various choices of the basic reproduction number $\mathcal{R}_0$ and of the volatility of opinions κ. In all panels the system is in the 'Partial Compliance' regime. We show both the effect of p in the ODE formulation (continuous line) and in the stochastic simulations run over an empirical two-layers network (dot-dashed line). Parameter values: $u = 5$, $q = 0.25$, $c = 0.3$, $p = 0.4$, $\varepsilon = 0.5$, and $x(0) = x_0 = 0.4$.

4. Conclusions

We build an SIS-based compartmental model that accounts for the simultaneous spread of the following: i) a pathogen on a network of physical contacts; and ii) opinions driving adoption of self-isolation on a network of social influence. By taking the coupled evolution of opinions and disease into account, we want to identify optimal implementations of the self-isolation measure combined with post-quarantine awareness.

The compartmental model that we propose allows for a partial adoption of the self-isolation measure, pre-isolation and post-isolation infections. In the compartment of infectious individuals who break quarantine, the infectiousness is assumed to be reduced as a consequence of an increased awareness, resulting in behaviors such as mask wearing or social distancing. The partial adoption of the measure refers to the binary choice that individuals make: to isolate or not to isolate. This decision is governed by an imitation dynamic and depends on a careful comparison of one's current decision with the one of the contacts. The costs of the two possible strategies are carefully weighted by the deciding individuals who are considered to behave rationally: a change of strategy only takes place if the opposite strategy would incur a lower cost. On the one hand, the cost of complying with the isolation measure is assumed to increase with the isolation duration and with the incurred cost. On the other hand, the cost of not complying arises from the state of the epidemic. The prevalence is often considered as the indicator of the state of an outbreak that affects the compliance of players in imitation dynamics models. However, the incidence rate is another standard indicator in epidemiology, and here, we study how this additional source of information can affect the dynamics of the coupled disease-behavior model. Instead of solely using the prevalence to assess the state of the epidemics, we model the cost of quarantine through a convex combination of prevalence and incidence.

We find that despite a seemingly complex intertwined behavior, the equilibria of the dynamics are fairly simple. There are two disease-free equilibria and three endemic equilibria that can be distinguished by the share of complying individuals in the stationary limit. The 'No Compliance' and the 'Full Compliance' endemic equilibria are stable when the cost of quarantine is too big or too small, respectively. In the regions of the parameter space where these equilibria are stable, the system collapses to a long-time state that is independent of the imitation dynamics. The third endemic equilibrium is characterized by a partial level of compliance in the population. This regime becomes particularly relevant in more optimistic scenarios, characterized by lower basic reproduction numbers, shorter delays to enter isolation (large u), and larger levels of caution after the isolation period (large ε). In this regime, the equilibrium prevalence reduces to the total cost to self-isolate, which is the product of the (relative) average time spent in isolation (through q) and the cost per time unit (through c) (see Equation (3.4)). In contrast, the equilibrium fraction of complying individuals decays with u and ε. Consequently, encouraging individuals to hurry into isolation and to stay cautious after exiting isolation allows to achieve the same level of disease circulation with fewer people complying, thus helping to relieve the social burden imposed by the implementation of the self-isolation measure.

In this work, we also address the well-known trade-off between the benefits of longer isolation periods and of widespread compliance in breaking chains of transmission. Within our framework, we are interested in seeing the conditions for the resolution of the imitation dynamics being governed by this vary trade-off. We find that there exists a duration able to minimize the equilibrium prevalence, given by the longest isolation duration that still allows full compliance of the population, at a given

cost of quarantine. The existence of this minimum implies that it is essential to reach high levels of adoption, even if this means that the isolation duration needs to be shortened. However, if the cost of isolation is too small, then it is always beneficial to have the longest isolation duration; alternatively, if the cost is too high, then increasing the isolation duration further than a certain point brings no benefit at all. Still, as expected, the equilibrium prevalence always becomes smaller, the lower the cost of quarantine. To summarize, in many settings, it is beneficial to shorten the isolation duration, while a lower cost of quarantine is always advantageous. Reducing the cost of quarantine can be achieved through incentives such as paid sick leave.

Although the parameter p that indicates the relative importance given to prevalence compared to the incidence rate plays no role on the equilibria nor on their stability conditions, it turns out that it may affect the transient phase of the dynamics. More specifically, either different choices of p give the same dynamics, or a lower p systematically gives a lower peak prevalence in the transient phase. We measure this effect both in the mean-field framework and on a multiplex network. We find that favoring the incidence rate as an indicator of the state of an outbreak might help limit the amplitude of an initial overshoot. Additionally, the observed advantages of incidence over prevalence become stronger the faster the dynamics (i.e., for a larger reproduction number and a larger volatility of opinions).

We test our analytical predictions against numerical simulations on an empirical multiplex network from the Copenhagen Network Study. Our mean-field results hold fairly.

This study comes with a set of limitations including the following: (i) the minimal design of a compartmental model counting a small number of compartments; (ii) the representation of how individuals access information about the state of the outbreak; (iii) the assumptions regarding how adoption of self-isolation spreads within the population; and (iv) the preliminary nature of our investigation of the impact of network structure on our predictions.

First off, for the sake of simplicity and so that we could draw analytically tractable conclusions, we have decided to work with a compartmental model - that comes with its own limitations - and we have opted for a limited amount of compartments. Being a compartmental model, we assumed a constant and homogeneous infectiousness and susceptibility of individuals. However, we incorporated a post-quarantine reduced infectiousness to partially account for a lower pathogen load at the end of the infectious period, though this reduced infectiousness is missing in the course of infection of individuals who do not comply. The rates of transition from one compartment to the next are assumed to be Poissonian, despite evidence that, for example, the infectious period follows more complex distributions [42, 43]. A more detailed modeling of the time spent in isolation could be obtained using age-structured partial differential equations (PDE); for instance, consider the time elapsed since the start of quarantine [61] or structure the population with respect to the pathogen load [62]. Apart from limitations that affect compartmental models in general, we opted for a limited amount of compartments to keep analytical derivations tractable and interpretable. For example, we decided to disregard the isolation of healthy individuals. Such a situation would be interesting to account for a more realistic toll of the isolation measure. Healthy individuals may indeed be asked to isolate from the community when preventive quarantine is implemented (e.g., because of the lack of accurate, widely distributed, and affordable diagnostic tests) instead of the self-isolation of only known cases treated in the present work. Moreover, we have not considered isolation periods that exceed the time for recovery needlessly, but as a consequence of the difficulty in estimating the end of the infectious period. In addition, in order to better describe the evolution of infectious diseases such as COVID-19, an exposed compartment

and a transitory removed compartment that accounts for temporary immunity are generally considered to be important [35, 37]. In this light, our model corresponds to a worst case scenario. Additionally, we disregarded the possibility for individuals to leave the dynamics as a consequence of death or of permanent measures such as vaccinations.

Second, we made some assumptions, on how information on the state of the outbreak is accessed; they should be examined in future work. To keep the model simple, the information about the state of the epidemic has been treated as memoryless, although some works have relaxed this assumption [63,64]. We assumed that individuals access real instantaneous values of the prevalence and of the incidence rate, and we completely disregarded delays or deviations from the actual values (e.g., due to cognitive biases and underdetection). If the underdetection is systematic, in our model, we would expect it to affect the effective rate of change of opinion and the cost of quarantine. Moreover, the addition of a compartment for hospitalized patients would allow one to account for the number of hospitalizations as an indicator of the severity of the outbreak and the saturation of health care [65]. Distinguishing between local and global information about the state of an outbreak would be interesting for a future analysis on networks [29, 66] or using a PDE approach [67]. Indeed, these frameworks could account for biases that arise from estimations of the severity or state of an outbreak based on observations made in people's local social environments and compare the effect of local and population-level information.

Third, our analysis has limitations concerning the way compliance is assumed to evolve in time. There is evidence that complex contagion better describes the propagation of opinions on social networks [68, 69]. In our model, the exposure to a single individual with opposite strategy is sufficient to allow someone to challenge its strategy. Additionally, our model disregards homophily, in particular homophily in the network of social influence [70]. We expect a threshold type of model and the introduction of homophily to reduce the parameter κ that accounts for the strategy update rate, but the phenomenology could change in more complex ways. We did not consider that individuals could spontaneously change their mind regarding the compliance with the control measure [26]. Moreover, as briefly discussed above, we considered that a change of opinion only affects individuals who have yet to decide whether to isolate or not. As a consequence, isolating individuals who change their opinion are assumed to not immediately exit quarantine. Instead, it would make sense to consider that individuals who change their mind during the isolation period could abort it. In this case, we expect that sustained oscillations would no longer be possible, which is similar to what was found for mask wearers [33].

Finally, we only performed a preliminary comparison of analytical predictions against stochastic simulations run on an empirical network. We did not perform any systematic analysis of the impact of different network structures on the transient and stationary parts of the dynamics for different values of the parameters. Our results suggest that the network structure affects our analytical predictions in the stationary limit and may affect the amplitude of observed oscillations (potentially as a consequence of weak multi-layer degree correlations). In the future, it would be important to check what network features are responsible for this discrepancy and whether specific network structures are able to affect the dependence of population-level quantities on the model parameters.

Acknowledgments

The authors first thank the organizing team of the event Current Challenges Workshop on Epidemic Modelling, Girona 2023, where they met and started to discuss the present work. The authors also thank PEPS-CNRS for funding the project, and François Castella for his critical look at the early stages of the model. GdM is grateful to the Institut Agro and the Irmar lab (France) for inviting her and HM to Gerardo Iñiguez and the Tampere Complexity Lab (Finland) for their hospitality. HM also acknowledges support of the 'Chair Modélisation Mathématique et Biodiversité (MMB)' of Veolia - Ecole polytechnique - Museum national d'Histoire naturelle - Fondation X, and of Sanofi through the FluCov project. Finally, the authors thank the two anonymous reviewers and the editor for their useful suggestions.

Use of AI tools declaration

The authors declare they have not used Artificial Intelligence (AI) tools in the creation of this article.

Conflict of interest

All authors declare no conflicts of interest in this paper.

Code availability

The Python codes used throughout this paper are available at the following GitHub repository: `https://github.com/Hugo-Martin/SIS-quarantine`.

References

1. M. Setbon, J. Raude, Factors in vaccination intention against the pandemic influenza a/h1n1, *European J. Public Health*, **20** (2010), 490–494. https://doi.org/10.1093/eurpub/ckq054
2. J. Raude, J.-M. Lecrique, L. Lasbeur, C. Leon, R. Guignard, E. du Roscoät, et al., Determinants of preventive behaviors in response to the covid-19 pandemic in france: Comparing the sociocultural, psychosocial, and social cognitive explanations, *Front. Psychol.*, **11** (2020). https://doi.org/10.3389/fpsyg.2020.584500
3. P. Peretti-Watel, V. Seror, S. Cortaredona, O. Launay, J. Raude, P. Verger, et al., Enquête Longitudinale, and for the Coronavirus and Confinement and COCONEL and Study Group, Attitudes about COVID-19 lockdown among general population, France, March 2020, *Emerg. Infect. Dis.*, **27** (2020), 301–303. https://doi.org/10.3201/eid2701.201377
4. S. Bartolo, E. Deliege, O. Mancel, P. Dufour, S. Vanderstichele, M. Roumilhac, et al., Determinants of influenza vaccination uptake in pregnancy: A large single-centre cohort study, *BMC Pregnancy Childb.*, **19** (2019). https://doi.org/10.1186/s12884-019-2628-5
5. S. C. Montgomery, M. Donnelly, P. Bhatnagar, A. Carlin, F. Kee, R. F. Hunter, Peer social network processes and adolescent health behaviors: A systematic review, *Prev. Med.*, **130** (2020), 105900. https://doi.org/10.1016/j.ypmed.2019.105900

6. A. Aghaeeyan, P. Ramazi, M. A. Lewis, Revealing decision-making strategies of americans in taking covid-19 vaccination, *Bull. Math. Biol.*, **86** (2024). https://doi.org/10.1007/s11538-024-01290-4
7. C. Betsch, F. Renkewitz, T. Betsch, C. Ulshöfer, The influence of vaccine-critical websites on perceiving vaccination risks, *J. Health Psychol.*, **15** (2010). https://doi.org/10.1177/1359105309353647
8. S. Funk, M. Salathé, V. Jansen, Modelling the influence of human behaviour on the spread of infectious diseases: A review, *J. R. Soc. Interface*, **7** (2010). https://doi.org/10.1098/rsif.2010.0142
9. S. Funk, S. Bansal, C. T. Bauch, K. T. Eames, W. J. Edmunds, A. P. Galvani, et al., Nine challenges in incorporating the dynamics of behaviour in infectious diseases models, *Epidemics*, **10** (2015), 21–25. https://doi.org/10.1016/j.epidem.2014.09.005
10. F. Verelst, L. Willem, P. Beutels, Behavioural change models for infectious disease transmission: A systematic review (2010–2015), *J. R. Soc. Interface*, **13** (2016), 20160820. https://doi.org/10.1098/rsif.2016.0820
11. S. L. Chang, M. Piraveenan, P. Pattison, M. Prokopenko, Game theoretic modelling of infectious disease dynamics and intervention methods: A review, *J. Biol. Dyn.*, **14** (2020), 57–89. https://doi.org/10.1080/17513758.2020.1720322
12. L. LeJeune, N. Ghaffarzadegan, L. M. Childs, O. Saucedo, Formulating human risk response in epidemic models: Exogenous vs endogenous approaches, *Eur. J. Oper. Res.*, **324** (2025), 246–258. https://doi.org/10.1016/j.ejor.2025.01.004
13. Z. Wang, M. A. Andrews, Z.-X. Wu, L. Wang, C. T. Bauch, Coupled disease–behavior dynamics on complex networks: A review, *Phys. Life Rev.*, **15** (2015), 1–29. https://doi.org/10.1016/j.plrev.2015.07.006
14. A. Reitenbach, F. Sartori, S. Banisch, A. Golovin, A. Calero Valdez, M. Kretzschmar, et al., Coupled infectious disease and behavior dynamics. A review of model assumptions, *Rep. Prog. Phys.*, **88** (2024), 016601. https://dx.doi.org/10.1088/1361-6633/ad90ef
15. D. Weston, K. Hauck, R. Amlôt, Infection prevention behaviour and infectious disease modelling: A review of the literature and recommendations for the future, *BMC Public Health*, **18** (2018), 336. https://doi.org/10.1186/s12889-018-5223-1
16. A. Hamilton, F. Haghpanah, A. Tulchinsky, N. Kipshidze, S. Poleon, G. Lin, et al., Incorporating endogenous human behavior in models of covid-19 transmission: A systematic scoping review, *Dialogues Health*, **4** (2024), 100179. https://doi.org/10.1016/j.dialog.2024.100179
17. J. Bedson, L. Skrip, D. Pedi, S. Abramowitz, S. Carter, M. Jalloh, et al., A review and agenda for integrated disease models including social and behavioural factors, *Nat. Hum. Behav.*, **5** (2021), 834–846. https://doi.org/10.1038/s41562-021-01136-2
18. A. D'Onofrio, P. Manfredi, *Modeling the Interplay Between Human Behavior and the Spread of Infectious Diseases*, Springer, 2013.https://doi.org/10.1007/978-1-4614-5474-8
19. J. Tanimoto, *Sociophysics approach to epidemics*, Evolutionary Economics and Social Complexity Science, Springer, Singapore, 2021. https://doi.org/10.1007/978-981-33-6481-3

20. K. S. Josef Hofbauer, *The theory of evolution and dynamical systems: Mathematical aspects of selection*, Cambridge Univ. Press, 1988.

21. C. T. Bauch, Imitation dynamics predict vaccinating behaviour, *Proc. R. Soc. B.*, **272** (2005), 1669–1675. https://doi.org/10.1098/rspb.2005.3153

22. T. Oraby, V. Thampi, C. T. Bauch, The influence of social norms on the dynamics of vaccinating behaviour for paediatric infectious diseases, *Proc. R. Soc. B Biol. Sci.*, **281** (2014), 20133172. https://doi.org/10.1098/rspb.2013.3172

23. S. L. Chang, M. Piraveenan, M. Prokopenko, The effects of imitation dynamics on vaccination behaviours in SIR-network model, *Int. J. Environ. Res. Public Health*, **16** (2019), 2477. https://doi.org/10.3390/ijerph16142477

24. Q. Yin, Z. Wang, C. Xia, C. T. Bauch, Impact of co-evolution of negative vaccine-related information, vaccination behavior and epidemic spreading in multilayer networks, *Commun. Nonlinear Sci. Numer. Simulat.*, **109** (2022), 106312. https://doi.org/10.1016/j.cnsns.2022.106312

25. M. M.-U.-R. Khan, J. Tanimoto, Influence of waning immunity on vaccination decision-making: A multi-strain epidemic model with an evolutionary approach analyzing cost and efficacy, *Infect. Dis. Model.*, **9** (2024), 657–672. https://doi.org/10.1016/j.idm.2024.03.004

26. P. Poletti, B. Caprile, M. Ajelli, A. Pugliese, S. Merler, Spontaneous behavioural changes in response to epidemics, *J. Theor. Biol.*, **260** (2009). https://doi.org/10.1016/j.jtbi.2009.04.029

27. S. Zhao, L. Stone, D. Gao, S. S. Musa, M. K. C. Chong, D. He, et al., Imitation dynamics in the mitigation of the novel coronavirus disease (covid-19) outbreak in Wuhan, China from 2019 to 2020, *Ann. Transl. Med.*, **8** (2020). https://doi.org/10.21037/atm.2020.03.168

28. N. T. Maia Martcheva, C. N. Ngonghala, Effects of social-distancing on infectious disease dynamics: An evolutionary game theory and economic perspective, *J. Biol. Dyn.*, **15** (2021), 342–366. https://doi.org/10.1080/17513758.2021.1946177

29. J. Cascante-Vega, S. Torres-Florez, J. Cordovez, M. Santos-Vega, How disease risk awareness modulates transmission: Coupling infectious disease models with behavioural dynamics, *R. Soc. Open Sci.*, **9** (2022), 210803. https://doi.org/10.1098/rsos.210803

30. A. Kabir, T. Risa, J. Tanimoto, Prosocial behavior of wearing a mask during an epidemic: An evolutionary explanation, *Sci. Rep.*, **11** (2021), 12621. https://doi.org/10.1038/s41598-021-92094-2

31. A. Traulsen, S. A. Levin, C. M. Saad-Roy, Individual costs and societal benefits of interventions during the Covid-19 pandemic, *Proc. Natl. Acad. Sci. U.S.A.*, **120** (2023), e2303546120. https://doi.org/10.1073/pnas.2303546120

32. M. Asfaw, B. Buonomo, S. Kassa, Impact of human behavior on itns control strategies to prevent the spread of vector borne diseases, *Atti. Accad. Pelorit. Pericol., Cl. Sci. Fis. Mat. Nat.*, **96** (2018), 2. https://doi.org/10.1478/AAPP.96S3A2

33. H. Martin, F. Castella, F. Hamelin, Wearing face masks to protect oneself and/or others: Counter-intuitive results from a simple epidemic model accounting for selfish and altruistic human behaviour, *submitted for publication*.

34. C. M. Peak, L. M. Childs, Y. H. Grad, C. O. Buckee, Comparing nonpharmaceutical interventions for containing emerging epidemics, *Proc. Natl. Acad. Sci. U.S.A.*, **114** (2017), 4023–4028. https://doi.org/10.1073/pnas.1616438114

35. R. Tori, J. Tanimoto, A study on prosocial behavior of wearing a mask and self-quarantining to prevent the spread of diseases underpinned by evolutionary game theory, *Chaos Soliton. Fract.*, **158** (2022), 112030. https://doi.org/10.1016/j.chaos.2022.112030

36. C. Eksin, J. S. Shamma, J. S. Weitz, Disease dynamics in a stochastic network game: A little empathy goes a long way in averting outbreaks, *Sci. Rep.*, **7** (2017), 44122. http://dx.doi.org/10.1038/srep44122

37. R. Zhang, B. Xie, Y. Kang, M. Liu, Modeling and analyzing quarantine strategies of epidemic on two-layer networks: Game theory approach, *J. Biol. Sys.*, **31** (2023), 21–35. https://doi.org/10.1142/S021833902350002X

38. G. de Meijere, V. Colizza, E. Valdano, C. Castellano, Effect of delayed awareness and fatigue on the efficacy of self-isolation in epidemic control, *Phys. Rev. E*, **104** (2021), 044316. https://doi.org/10.1103/PhysRevE.104.044316

39. H. Hethcote, M. Zhien, L. Shengbing, Effects of quarantine in six endemic models for infectious diseases, *Math. Biosci.*, **180** (2002), 141–160. https://doi.org/10.1016/S0025-5564(02)00111-6

40. S. Chen, M. Small, X. Fu, Global stability of epidemic models with imperfect vaccination and quarantine on scale-free networks, *IEEE Trans. Netw. Sci. Eng.*, **7** (2019), 1583–1596. https://doi.org/10.1109/TNSE.2019.2942163

41. A. Petherick, R. Goldszmidt, E. B. Andrade, R. Furst, T. Hale, A. Pott, et al., A worldwide assessment of changes in adherence to covid-19 protective behaviours and hypothesized pandemic fatigue, *Nat. Hum. Behav.*, **5** (2021), 1145–1160. https://doi.org/10.1038/s41562-021-01181-x

42. X. He, E. H. Y. Lau, P. Wu, X. Deng, J. Wang, X. Hao, et al., Temporal dynamics in viral shedding and transmissibility of COVID-19, *Nat. Med.*, **26** (2020), 672–675. https://doi.org/10.1038/s41591-020-0869-5 .

43. A. Marc, M. Kerioui, F. Blanquart, J. Bertrand, O. Mitjà, M. Corbacho-Monné, et al., Quantifying the relationship between sars-cov-2 viral load and infectiousness, *eLife*, **10** (2021), e69302. https://doi.org/10.7554/eLife.69302

44. P. J. White, Mathematical models in infectious disease epidemiology, in *Infect. Dis. (Fourth Edition)* (eds. J. Cohen, W. G. Powderly and S. M. Opal), fourth edition edition. Elsevier, 2017, 49–53. https://doi.org/10.1016/B978-0-7020-6285-8.00005-8

45. P.-A. Bliman, A. Carrozzo-Magli, A. D'Onofrio, P. Manfredi, Tiered social distancing policies and epidemic control, *Proc. R. Soc. A*, **478** (2022). https://doi.org/10.1098/rspa.2022.0175

46. M. A. Amaral, M. M. de Oliveira, M. A. Javarone, An epidemiological model with voluntary quarantine strategies governed by evolutionary game dynamics, *Chaos Soliton. Fract.*, **143** (2021), 110616. https://doi.org/10.1016/j.chaos.2020.110616

47. R. M. Anderson, R. M. May, *Infectious Diseases of Humans: Dynamics and Control*, Oxford University Press, 1991.

48. L.-S. Young, S. Ruschel, S. Yanchuk, T. Pereira, Consequences of delays and imperfect implementation of isolation in epidemic control, *Sci. Rep.*, **9** (2019), 3505. https://doi.org/10.1038/s41598-019-39714-0

49. X.-B. Zhang, H.-F. Huo, H. Xiang, Q. Shi, D. Li, The threshold of a stochastic siqs epidemic model, *Phys. A*, **482** (2017), 362–374. https://doi.org/10.1016/j.physa.2017.04.100

50. M. Mancastroppa, R. Burioni, V. Colizza, A. Vezzani, Active and inactive quarantine in epidemic spreading on adaptive activity-driven networks, *Phys. Rev. E*, **102** (2020), 020301. https://doi.org/10.1103/PhysRevE.102.020301

51. M. N. Mbah, J. Liu, C. Bauch, Y. Tekel, J. Medlock, L. A. Meyers, et al., The impact of imitation on vaccination behavior in social contact networks, *PLoS Comput. Biol.*, **8** (2012), e1002469. https://doi.org/10.1371/journal.pcbi.1002469

52. P. van den Driessche, Reproduction numbers of infectious disease models, *Infect. Dis. Model.*, **2** (2017), 288–303. http://dx.doi.org/10.1016/j.idm.2017.06.002

53. Y. Alimohamadi, M. Taghdir, M. Sepandi, Estimate of the basic reproduction number for covid-19: A systematic review and meta-analysis, *J. Prev. Med. Public Health*, **53** (2020), 151–157. http://dx.doi.org/10.3961/jpmph.20.076

54. D. Leith, C. L'Orange, J. Volckens, Quantitative protection factors for common masks and face coverings, *Environ. Sci. Technol.*, **55** (2021), 3136–3143. https://doi.org/10.1021/acs.est.0c07291

55. X. Q. Koh, A. Sng, J. Y. Chee, A. Sadovoy, P. Luo, D. Daniel, Outward and inward protection efficiencies of different mask designs for different respiratory activities, *Aerosol. Sci.*, **160** (2022), 105905. https://doi.org/10.1016/j.jaerosci.2021.105905

56. W. Cota, S. C. Ferreira, Optimized gillespie algorithms for the simulation of markovian epidemic processes on large and heterogeneous networks, *Comput. Phys. Commun.*, **219** (2017). https://doi.org/10.1016/j.cpc.2017.06.007

57. S. C. Ferreira, C. Castellano, R. Pastor-Satorras, Epidemic thresholds of the susceptible-infected-susceptible model on networks: A comparison of numerical and theoretical results, *Phys. Rev. E*, **86** (2012), 041125. https://doi.org/10.1103/PhysRevE.86.041125

58. Z. Qiu, B. Espinoza, V. V. Vasconcelos, C. Chen, S. M. Constantino, S. A. Crabtree, et al., Understanding the coevolution of mask wearing and epidemics: A network perspective, *Proc. Natl. Acad. Sci. U.S.A.*, **119** (2022), e2123355119. http://dx.doi.org/10.1073/pnas.2123355119

59. P. Sapiezynski, A. Stopczynski, D. D. Lassen, S. Lehmann, Interaction data from the copenhagen networks study, *Sci. Data*, **6** (2019), 315. https://doi.org/10.1038/s41597-019-0325-x

60. T. P. Peixoto, The netzschleuder network catalogue and repository, 2020, Available from: `https://networks.skewed.de/`

61. F. Wu, X. Liang, J. Lei, Modelling Covid-19 epidemic with confirmed cases-driven contact tracing quarantine, *Infect. Dis. Model.*, **8** (2023), 415–426. https://doi.org/10.1016/j.idm.2023.04.001

62. R. Della Marca, N. Loy, A. Tosin, An SIR model with viral load-dependent transmission, *J. Math. Biol.*, **86** (2023), 61. https://doi.org/10.1007/s00285-023-01901-z

63. A. d'Onofrio, P. Manfredi, E. Salinelli, Vaccinating behaviour, information, and the dynamics of sir vaccine preventable diseases, *Theor. Popul. Biol.*, **71** (2007). https://doi.org/10.1016/j.tpb.2007.01.001

64. Y. N. Kyrychko, K. B. Blyuss, Vaccination games and imitation dynamics with memory, *Chaos*, **33** (2023), 033134. https://doi.org/10.1063/5.0143184

65. P. Verma, V. Kumar, S. Bhattacharyya, Modelling behavioural interactions in infection disclosure during an outbreak: An evolutionary game theory approach, *Math. Biosci. Eng.*, **22** (2025), 1931–1955. https://doi.org/10.3934/mbe.2025070

66. D. H. Silva, C. Anteneodo, S. C. Ferreira, Epidemic outbreaks with adaptive prevention on complex networks, *Commun. Nonlinear Sci. Numer. Simulat.*, **116** (2023), 106877. https://doi.org/10.1016/j.cnsns.2022.106877

67. M. Banerjee, V. Volpert, P. Manfredi, A. d'Onofrio, Behavior-induced phase transitions with far from equilibrium patterning in a sis epidemic model: Global vs non-local feedback, *Phys. D*, **469** (2024), 134316. https://doi.org/10.1016/j.physd.2024.134316

68. B. Mønsted, P. Sapieżyński, E. Ferrara, S. Lehmann, Evidence of complex contagion of information in social media: An experiment using twitter bots, *PLoS ONE*, **12** (2017), e0184148. https://doi.org/10.1371/journal.pone.0184148

69. D. A. Sprague, T. House, Evidence for complex contagion models of social contagion from observational data, *PLoS ONE*, **12** (2017), e0180802. https://doi.org/10.1371/journal.pone.0180802

70. Z. He, C. T. Bauch, Effect of homophily on coupled behavior-disease dynamics near a tipping point, *Math. Biosci.*, **376** (2024), 109264. https://doi.org/10.1016/j.mbs.2024.109264

71. L. Allen, *An Introduction to Mathematical Biology*, Pearson/Prentice Hall, 2007.

A. Recovery from U, Q, I and F occurs with the same rate

Individuals in compartment Q can recover through two *alternative* paths: $Q \to S$ and $Q \to F \to S$. Let t_S be the time for the event $Q \to S$ and t_F be the time for the event $Q \to F$. The probability that the path $Q \to S$ is chosen is as follows:

$$P(t_S < t_F) = P(t_S = t)P(t_F > t),$$

where $P(t_S = t) = \mu e^{-\mu t}$ and

$$P(t_F > t) = \int_t^\infty \mu_Q e^{-\mu_Q s}\,\mathrm{d}s = e^{-\mu_Q t}.$$

Similarly, the probability that the path $Q \to F$ is chosen is as follows:

$$P(t_F < t_S) = \mu_Q e^{-\mu_Q t} e^{-\mu t}.$$

The normalization of $P(t_S < t_F)$ is as follows:

$$N_S = \int_0^\infty \mu e^{-(\mu+\mu_Q)t}\,\mathrm{d}t = \frac{\mu}{\mu+\mu_Q},$$

while, the normalization of $P(t_F < t_S)$ is as follows:

$$N_F = \int_0^\infty \mu_Q e^{-(\mu+\mu_Q)t}\,\mathrm{d}t = \frac{\mu_Q}{\mu+\mu_Q}.$$

Thus, the average time taken to recover through the direct recovery path $Q \to S$ is as follows:

$$\begin{aligned}\tau_{Q\to S} &= \int_0^\infty t\frac{P(t_S = t)P(t_F > t)}{N_S}dt,\\ &= \int_0^\infty (\mu+\mu_Q)te^{-(\mu+\mu_Q)t}dt,\\ &= \frac{1}{\mu+\mu_Q},\end{aligned}$$

where we performed an integration by parts in the last step. This average time is the same as the one of the transition $Q \to F$. Thus, the average time spent in isolation is also $\frac{1}{\mu+\mu_Q}$. This is because the sharpest exponential dominates the other one, whether it be the one of the $Q \to S$ or of the $Q \to F$ transition. The probability of the $Q \to S$ transition is as follows:

$$p_{Q\to S} = \int_0^\infty P(t_S = t)P(t_F > t)dt = N_S = \frac{\mu}{\mu+\mu_Q}.$$

For the $Q \to F$ transition, it is instead as follows:

$$p_{Q\to F} = \int_0^\infty P(t_F = t)P(t_S > t)dt = N_F = \frac{\mu_Q}{\mu+\mu_Q}.$$

Therefore,

$$\begin{aligned}\tau = \tau_{Q\to S}p_{Q\to S} + \tau_{Q\to F\to S}p_{Q\to F\to S} &= \frac{1}{\mu+\mu_Q}\frac{\mu}{\mu+\mu_Q} + \left(\frac{1}{\mu+\mu_Q}+\frac{1}{\mu}\right)\frac{\mu_Q}{\mu+\mu_Q},\\ &= \frac{1}{\mu},\end{aligned}$$

where the average time for the recovery of individuals in compartment Q is simply the average time of a Poissonian transition with rate μ. The same reasoning can be repeated for compartment U, which also shows multiple alternative paths to recovery. In this way, the average time of recovery of $I_{\text{tot}} = U + Q + I + F$ is also $1/\mu$, as expected for an SIS model.

B. Stability of the fixed points

We begin this section by recalling the Routh-Hurwitz criteria, specified for polynomials of order 3 and 5, that we will use to prove the local asymptotic stability of the EFC and EPC equilibria.

B.1. Routh-Hurwitz criteria

Lemma 1 (Routh-Hurwitz Conditions for Orders 3 and 5 [71])**.** *Let the monic real polynomial $P(\lambda) = \lambda^n + \alpha_1\lambda^{n-1} + \cdots + \alpha_{n-1}\lambda + \alpha_n$ be given. Then, $P(\lambda)$ is Hurwitz stable, that is, all roots have strictly negative real parts if and only if the following conditions hold:*

For $n = 3$***:***

$$\begin{cases} \alpha_1 > 0, \\ \alpha_3 > 0, \\ \alpha_1\alpha_2 > \alpha_3. \end{cases}$$

For $n = 5$***:***

$$\begin{cases} \alpha_i > 0, \textit{ for } i \in \{1,2,3,4,5\} \\ \alpha_1\alpha_2\alpha_3 > \alpha_3^2 + \alpha_1^2\alpha_4, \\ (\alpha_1\alpha_4 - \alpha_5)(\alpha_1\alpha_2\alpha_3 - \alpha_3^2 - \alpha_1^2\alpha_4) > \alpha_5(\alpha_1\alpha_2 - \alpha_3)^2 + \alpha_1\alpha_5^2. \end{cases}$$

These algebraic conditions are necessary and sufficient for the roots of $P(\lambda)$ *to lie entirely in the open left-half of the complex plane.*

B.2. Jacobian matrix

To assess the stability of each endemic equilibrium, we compute the jacobian matrix $J_{\mathcal{E}} =$

$$\begin{pmatrix} \frac{\mathcal{R}_0}{\mathcal{R}_{x^*}} - \mathcal{R}_{x^*} & 0 & -\frac{\mathcal{R}_0}{\mathcal{R}_{x^*}} & -\varepsilon\frac{\mathcal{R}_0}{\mathcal{R}_{x^*}} & 0 \\ \frac{\mathcal{R}_0}{\mathcal{R}_{x^*}} - \mathcal{R}_{x^*} + 1 & -(1+u) & -\frac{\mathcal{R}_0}{\mathcal{R}_{x^*}} & -\varepsilon\frac{\mathcal{R}_0}{\mathcal{R}_{x^*}} & 0 \\ 0 & ux^* & -(1+q) & 0 & \frac{u}{1+u}\left(1 - \frac{1}{\mathcal{R}_{x^*}}\right) \\ 0 & 0 & q & -1 & 0 \\ \kappa x^*(1-x^*)\left[1 + (1-p)\left(\frac{\mathcal{R}_0}{\mathcal{R}_{x^*}} - \mathcal{R}_{x^*}\right)\right] & 0 & -\kappa x^*(1-x^*)(1-p)\frac{\mathcal{R}_0}{\mathcal{R}_{x^*}} & -\varepsilon\kappa x^*(1-x^*)(1-p)\frac{\mathcal{R}_0}{\mathcal{R}_{x^*}} & \kappa(1-2x^*)\left[1 - \frac{1}{\mathcal{R}_{x^*}} - \frac{c}{1+q}\right] \end{pmatrix}.$$

and specify its values based on $\mathcal{E} \in \{\text{ENC}, \text{EPC}, \text{EFC}\}$ (i.e., $x^* = 0$, $x^* = 1$, or in-between).

B.3. Disease-free fixed points of the dynamics

For the two disease-free equilibria, we recover classical conditions: they always exist, and the DFNC is locally asymptotically stable if $\mathcal{R}_0 \leqslant 1$ (the special case $\mathcal{R}_0 = 1$ being dealt with by hand), while the DFFC is never stable.

B.4. Endemic fixed points of the dynamics

B.4.1. ENC equilibrium

For the ENC equilibrium, the Jacobian matrix reduces to the following:

$$\begin{pmatrix} 1 - \mathcal{R}_0 & 0 & -1 & -\varepsilon & 0 \\ 2 - \mathcal{R}_0 & -(1+u) & -1 & -\varepsilon & 0 \\ 0 & 0 & -(1+q) & 0 & \frac{u}{1+u}\left(1 - \frac{1}{\mathcal{R}_0}\right) \\ 0 & 0 & q & -1 & 0 \\ 0 & 0 & 0 & 0 & \kappa\left[1 - \frac{1}{\mathcal{R}_0} - \frac{c}{1+q}\right], \end{pmatrix},$$

which is a block-triangular matrix, and its associated characteristic polynomial is as follows:

$$P(\lambda) = (1 - \mathcal{R}_0 + \lambda)(1 + u + \lambda)(1 + \lambda)(1 + q + \lambda)\left(\kappa\left[1 - \frac{1}{\mathcal{R}_0} - \frac{c}{1+q}\right] - \lambda\right).$$

It yields two conditions for local asymptotic stability, namely $\mathcal{R}_0 > 1$ and

$$1 - \frac{1}{\mathcal{R}_0} < \frac{c}{1+q}.$$

B.4.2. EFC equilibrium

For the EFC equilibrium, the Jacobian matrix instead reads as follows:

$$\begin{pmatrix} \frac{\mathcal{R}_0}{\mathcal{R}_1} - \mathcal{R}_1 & 0 & -\frac{\mathcal{R}_0}{\mathcal{R}_1} & -\varepsilon\frac{\mathcal{R}_0}{\mathcal{R}_1} & 0 \\ \frac{\mathcal{R}_0}{\mathcal{R}_1} - \mathcal{R}_1 + 1 & -(1+u) & -\frac{\mathcal{R}_0}{\mathcal{R}_1} & -\varepsilon\frac{\mathcal{R}_0}{\mathcal{R}_1} & 0 \\ 0 & u & -(1+q) & 0 & \frac{u}{1+u}\left(1 - \frac{1}{\mathcal{R}_1}\right) \\ 0 & 0 & q & -1 & 0 \\ 0 & 0 & 0 & 0 & -\kappa\left[1 - \frac{1}{\mathcal{R}_1} - \frac{c}{1+q}\right] \end{pmatrix},$$

and developing with respect to the last row provides the stability condition

$$1 - \frac{1}{\mathcal{R}_1} > \frac{c}{1+q}.$$

The rest of the spectrum is given by computing the determinant

$$\begin{vmatrix} \frac{\mathcal{R}_0}{\mathcal{R}_1} - \mathcal{R}_1 - \lambda & 0 & -\frac{\mathcal{R}_0}{\mathcal{R}_1} & -\varepsilon\frac{\mathcal{R}_0}{\mathcal{R}_1} \\ \frac{\mathcal{R}_0}{\mathcal{R}_1} - \mathcal{R}_1 + 1 & -(1+u+\lambda) & -\frac{\mathcal{R}_0}{\mathcal{R}_1} & -\varepsilon\frac{\mathcal{R}_0}{\mathcal{R}_1} \\ 0 & u & -(1+q+\lambda) & 0 \\ 0 & 0 & q & -1-\lambda \end{vmatrix},$$

which can be processed, for instance, by applying the following operations:

1. L1 $\longleftarrow$ L1 - L2 - L3 - L4,
2. Factorization of $-(1+\lambda)$ in the first row,
3. $\forall j \in \{2,3,4\}$, Cj $\longleftarrow$ Cj + C1,
4. Developing along the first row,
5. L1 $\longleftarrow$ L1 - $\frac{1-\mathcal{R}_1}{q}$L3,

to obtain

$$\begin{aligned} &-(1+\lambda)\times \begin{vmatrix} \mathcal{R}_1 - \frac{\mathcal{R}_0}{\mathcal{R}_1} - u - \lambda & 0 & (1-\varepsilon)\frac{\mathcal{R}_0}{\mathcal{R}_1} + (1-\mathcal{R}_1) + \frac{1-\mathcal{R}_1}{q}(1+\lambda) \\ u & -(1+q+\lambda) & 0 \\ 0 & q & -(1+\lambda) \end{vmatrix}, \\ &= (1+\lambda)\times \\ &\left[\left(\mathcal{R}_1 - \frac{\mathcal{R}_0}{\mathcal{R}_1} + u + \lambda\right)(1+q+\lambda)(1+\lambda) - uq\left((1-\mathcal{R}_1) + (1-\varepsilon)\frac{\mathcal{R}_0}{\mathcal{R}_1} + \frac{1-\mathcal{R}_1}{q}(1+\lambda)\right)\right], \end{aligned}$$

using the rule of Sarrus.

We aim to apply the Routh-Hurwitz criterion to prove that all roots have a negative real part. Developing the polynomial in the brackets, we obtain $P(\lambda) = \lambda^3 + \alpha_1\lambda^2 + \alpha_2\lambda + \alpha_3$ with

– $\alpha_1 = \mathcal{R}_1 - \frac{\mathcal{R}_0}{\mathcal{R}_1} + u + q$,
– $\alpha_2 = \mathcal{R}_1(u+q) - \frac{\mathcal{R}_0}{\mathcal{R}_1}(q+1) + uq = \mathcal{R}_1(u+q) - \frac{\mathcal{R}_0}{\mathcal{R}_1}(q+1) + uq$,
– $\alpha_3 = \left(\mathcal{R}_1 - \frac{\mathcal{R}_0}{\mathcal{R}_1} + u - 1\right)q + (u-1)(q-1)\left[(\mathcal{R}_1 - 1)\frac{q}{q-1} - (1-\varepsilon)\frac{\mathcal{R}_0}{\mathcal{R}_1}\right]$.

We need to check that $\alpha_1 > 0$, $\alpha_3 > 0$, and $\alpha_1\alpha_2 > \alpha_3$. The first positivity is readily obtained by observing that

$$\frac{\mathcal{R}_0}{\mathcal{R}_1} = \frac{(u+1)(q+1)}{(u+1)(q+1) - u(1+\varepsilon q)} \leqslant u+1,$$

combined with $\mathcal{R}_1 > 1$. The second is obtained by computing the following:

$$\begin{aligned}\alpha_3 &= \mathcal{R}_1(u+1)(q+1) - \frac{\mathcal{R}_0}{\mathcal{R}_1}(q+1+(1-\varepsilon)uq),\\ &= (u+1)(q+1)\left(\mathcal{R}_1 - \frac{q+1+(1-\varepsilon)uq}{(u+1)(q+1) - u(1+\varepsilon q)}\right),\\ &= (u+1)(q+1)(\mathcal{R}_1 - 1),\end{aligned}$$

so positivity is obtained by the condition $\mathcal{R}_1 > 1$. Finally, we show the last inequality be rewriting the following:

$$\alpha_1 = \left(u + 1 - \frac{\mathcal{R}_0}{\mathcal{R}_1}\right) + \mathcal{R}_1 + q + 1 \qquad \text{and} \qquad \alpha_2 = (q+1)\mathcal{R}_1 + (q+2)\left(u + 1 - \frac{\mathcal{R}_0}{\mathcal{R}_1}\right) + (u+1)(\mathcal{R}_1 - 1),$$

which are both sums of three non-negative terms, with the product of the last of each being exactly α_3.

B.4.3. EPC equilibrium

To assess local stability, we have to study the negativity of the roots of the following:

$$\begin{vmatrix} \mathcal{R}_{x^*} - \frac{\mathcal{R}_0}{\mathcal{R}_{x^*}} - \lambda & 0 & -\frac{\mathcal{R}_0}{\mathcal{R}_{x^*}} & -\varepsilon\frac{\mathcal{R}_0}{\mathcal{R}_{x^*}} & 0 \\ 1 + \mathcal{R}_{x^*} - \frac{\mathcal{R}_0}{\mathcal{R}_{x^*}} & -(1+u+\lambda) & -\frac{\mathcal{R}_0}{\mathcal{R}_{x^*}} & -\varepsilon\frac{\mathcal{R}_0}{\mathcal{R}_{x^*}} & 0 \\ 0 & ux^* & -(1+q+\lambda) & 0 & \frac{u}{1+u}\left(1 - \frac{1}{\mathcal{R}_{x^*}}\right) \\ 0 & 0 & q & -(1+\lambda) & 0 \\ \kappa X\left[p + (1-p)(1 - \mathcal{R}_{x^*} + \frac{\mathcal{R}_0}{\mathcal{R}_{x^*}})\right] & 0 & -\kappa X\frac{1-p}{\mathcal{R}_{x^*}} & -\varepsilon\kappa X\frac{1-p}{\mathcal{R}_{x^*}} & -\lambda \end{vmatrix},$$

with $X = x^*(1-x^*) > 0$. First, we perform the following:

1. C4 $\longleftarrow$ C4 - ε C3,
2. L2 $\longleftarrow$ L2 - L1,

then we develop with respect to the last column to obtain the associated characteristic polynomial (up to the sign) as follows:

$$P(\lambda) = \lambda D_4(\lambda) + \kappa\frac{u}{1+u}\left(1 - \frac{1}{\mathcal{R}_{x^*}}\right)\frac{\mathcal{R}_0}{\mathcal{R}_{x^*}}XD_3(\lambda),$$

with $D_4(\lambda)$ and $D_3(\lambda)$ being the resulting 4×4 determinants, which leads to polynomials in λ of degree 4 and 3, respectively. Then, we compute the following:

$$D_4(\lambda) = \begin{vmatrix} \mathcal{R}_{x^*} - \frac{\mathcal{R}_0}{\mathcal{R}_{x^*}} - \lambda & 0 & -\frac{\mathcal{R}_0}{\mathcal{R}_{x^*}} & 0 \\ 1+\lambda & -(1+u+\lambda) & 0 & 0 \\ 0 & ux^* & -(1+q+\lambda) & \varepsilon(1+q+\lambda) \\ 0 & 0 & q & -(1+\varepsilon q+\lambda) \end{vmatrix},$$

$$= \begin{vmatrix} \mathcal{R}_{x^*} - \frac{\mathcal{R}_0}{\mathcal{R}_{x^*}} - \lambda & 0 & -\frac{\mathcal{R}_0}{\mathcal{R}_{x^*}} & 0 \\ 1+\lambda & -(1+u+\lambda) & 0 & 0 \\ 0 & ux^* & -(1+\lambda) & -(1-\varepsilon)(1+\lambda) \\ 0 & 0 & q & -(1+\varepsilon q+\lambda) \end{vmatrix},$$

$$= (1+\lambda)[\lambda^3 + (\frac{\mathcal{R}_0}{\mathcal{R}_{x^*}} - \mathcal{R}_{x^*} + u + q + 2)\lambda^2 + \left(\frac{\mathcal{R}_0}{\mathcal{R}_{x^*}} u x^* + \left(\frac{\mathcal{R}_0}{\mathcal{R}_{x^*}} - \mathcal{R}_{x^*}\right)(u+q+2) + (1+u)(1+q)\right)\lambda + \frac{\mathcal{R}_0}{\mathcal{R}_{x^*}} u x^*(1+\varepsilon q) + \left(\frac{\mathcal{R}_0}{\mathcal{R}_{x^*}} - \mathcal{R}_{x^*}\right)(1+u)(1+q)],$$

and straightforwardly apply the Routh-Hurwitz criterion to the polynomial in the brackets. As a result, all roots of D_4 have negative real parts. Some additional computations lead to the following:

$$D_3(\lambda) = (1-p)\frac{\mathcal{R}_0}{\mathcal{R}_{x^*}}(1+\varepsilon q+\lambda)\left(\frac{\mathcal{R}_0}{\mathcal{R}_{x^*}} - \mathcal{R}_{x^*} + \lambda\right)(1+u+\lambda),$$

which has three negative roots. For any $\kappa > 0$, all coefficients that appear in P are positive; thus, for sufficiently small positive perturbations of $\lambda D_4(\lambda)$ by the other term of P, the two last conditions to check in the Routh-Hurwith criterion still hold. As a result, all roots of P have negative real parts at least for a sufficiently small $\kappa > 0$. The code provided as a companion for this proof explicitly computes the critical bound above which the local asymptotic stability is not guaranteed. Additionally, the code displays two plots of the temporal dynamics of the x variable: one for a κ lying 5% below the critical value and the other 5% above. The former converges to a single value, whereas the latter exhibits sustained oscillations.

C. Impact of imitation on the dynamics

C.1. Equilibrium prevalence

When the imitation is completely turned off, our model collapses to the IDF model and the disease prevalence equation in the stationary limit reads as follows:

$$I^*_{\text{tot}}(p_Q) := 1 - \frac{1}{\mathcal{R}_{p_Q}},$$

with

$$\mathcal{R}_{p_Q} := \left(1 - \frac{u}{1+u}\frac{1+\varepsilon q}{1+q}p_Q\right)\mathcal{R}_0,$$

which is analogous to Equation 3.3, if we have a fixed compliance p_Q instead of the equilibrium compliance x^* that depends on the model parameters.

This suggests that, whether a coupled disease and opinion dynamics would yield a higher or lower equilibrium prevalence compared to the same disease model without opinion dynamics uniquely depends on the comparison between p_Q (the population baseline compliance) and x^*. In general, an imitation dynamic or self-regulation provides better epidemiological results as long as we are in the

regions of parameter space where $x^* > p_Q$ is satisfied. When a population has very low adoption levels, it is better for people to get exposed to information such as prevalence and incidence to have a chance to increase the overall compliance and improve mitigation. Instead, when a population has a very large baseline level of adoption, it is advantageous for people to not rethink their behavior to maintain high levels of compliance.

C.2. Transient prevalence

Although there is a discontinuity in the equilibrium prevalence between the limit case $\kappa = 0$ treated in the IDF model and the case $\kappa > 0$ studied in the present work, we see that this discontinuity arises in the following way from a common initial condition.

When $\kappa = 0$, the dynamics initially follows the trajectory predicted by the IDF model with $p_Q = x(t = 0)$ given by the initial condition. However, as soon as $\kappa > 0$, the long-time regime is characterized by a convergence to the trajectory predicted by IDF with $p_Q = x^*$. Further increasing κ anticipates the moment in which the initial condition is forgotten by the system and the system collapses onto its long-time trajectory. Thus, we find that despite the fact that the volatility κ of opinions does not contribute to the equilibria, it affects the transient phase.

Moreover, if the initial condition $x_0 < x^*$ (or the reverse $x_0 > x^*$), then the IDF model predicts $I_{\text{tot}}(p_Q = x_0) > I_{\text{tot}}(p_Q = x^*)$ (or the reverse $I_{\text{tot}}(p_Q = x_0) < I_{\text{tot}}(p_Q = x^*)$). This has a straighforward implication on the effect of κ on the transient phase: if $x_0 < x^*$ (or the reverse $x_0 > x^*$) then a lower cumulative number of infected individuals is achieved when the volatility κ is high (low).

See Figure 6 for a representative example of the effect of κ on the transient phase of the dynamics.

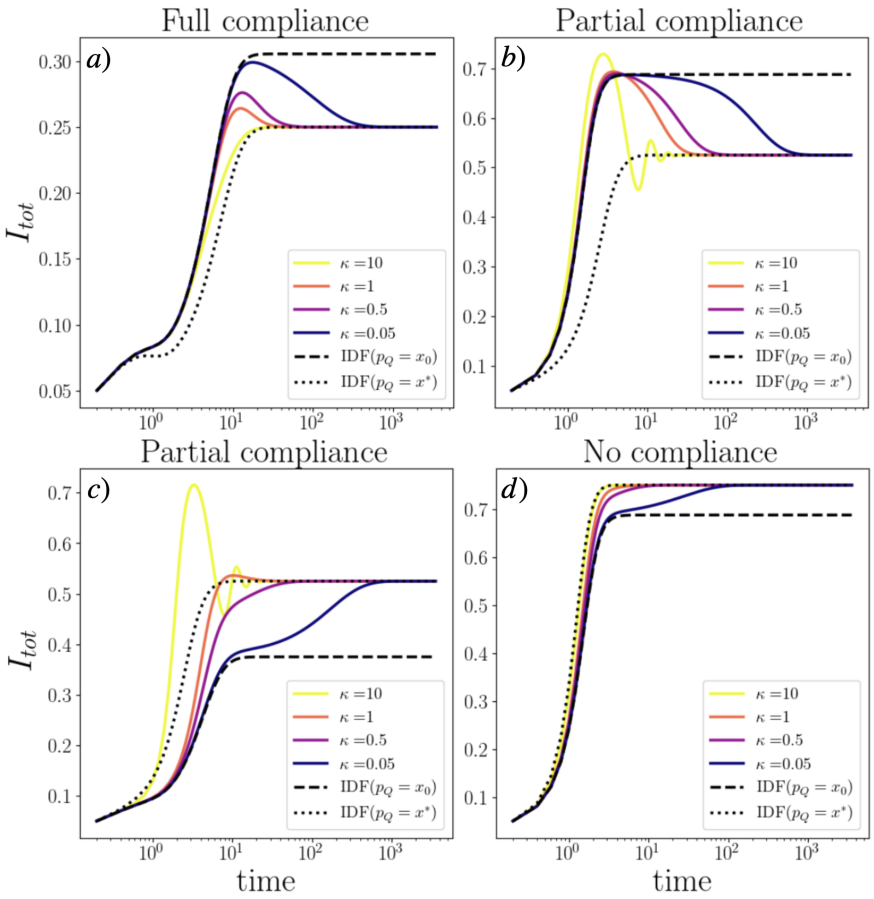

Figure 6. Effect of κ on the transient phase, in the EFC, EPC, and ENC regimes. Evolution of the prevalence in time with $x(0) = x_0$ the initial condition on the fraction of cooperators. We distinguish between the scenarios with $x_0 < x^*$ ('Full compliance' and 'Partial compliance') and those with $x_0 > x^*$ ('Partial compliance' and 'No compliance'). Parameter values: $\mathcal{R}_0 = 4$, $\varepsilon = 0.2$, $\mu = 1$, $\mu_U = 5$, and $\mu_Q = 1/3$. In 'No Compliance': $x_0 = 0.3$ and $c = 2$; in 'Partial Compliance': $x_0 = 0.3$ and $c = 0.7$ (top, right) or $x_0 = 0.9$ and $c = 0.7$ (bottom, left) ; and in 'Full Compliance': $x_0 = 0.96$ and $c = 0.1$.

C.3. Optimal isolation duration with and without imitation dynamics

In the model with imitation dynamics, the compliance takes a negative contribution given by the average duration of the isolation period (the payoff π_Q of isolating). In Figure 7, we compare the $\kappa > 0$ case (main text) with the $\kappa = 0$ limit but such that the level of adoption is a decaying function of the isolation duration (similarly to [38]). This coupling between the level of adoption and the isolation duration allows the $q \to 0$ limit of very long quarantines to be associated with a larger prevalence than in the case without coupling. This yields an optimal isolation duration in the entire space of parameters when $\kappa = 0$, which is not observed when $\kappa > 0$.

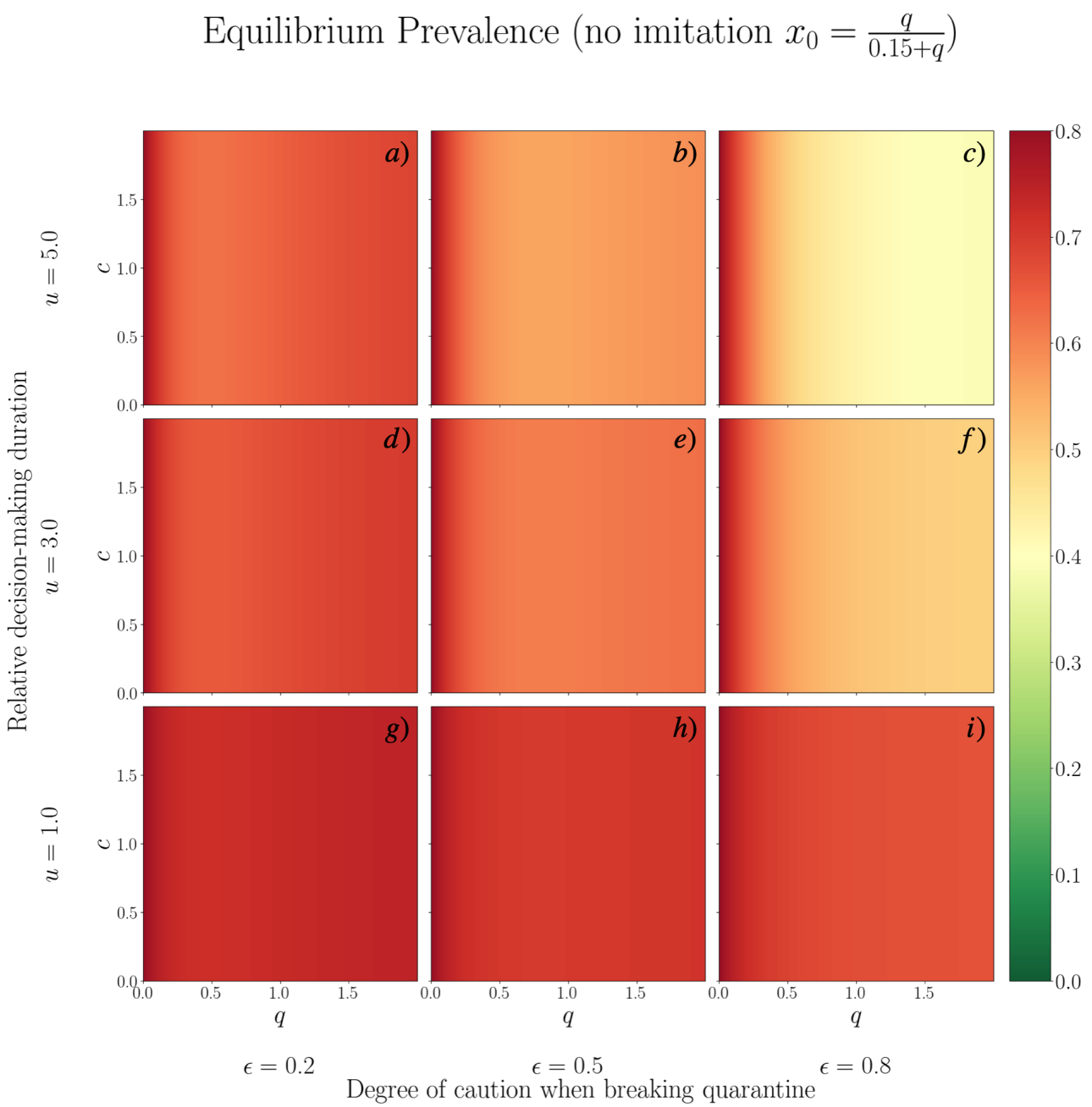

Figure 7. Equilbrium prevalence in the absence of imitation dynamics but with compliance that decays with the duration of isolation. Heatmap of the equilibrium prevalence depending on the cost c of quarantine, the lack of coverage q of the infectious period by quarantine, the celerity of entrance in isolation u, and the degree of caution ε when breaking quarantine. We assumed that the compliance p_Q decays as $q/(0.15 + q)$, which is similar to the minimal assumption made in [38]. Parameters: $\mathcal{R}_0 = 5$ and $x(0) = x_0 = 0.8$.

AIMS Press